RESEARCH ARTICLE





The effect of repeated hurricanes on the age of organic carbon in humid tropical forest soil

Allegra C. Mayer^{1,2,3} | Karis J. McFarlane² | Whendee L. Silver¹

¹Department of Environmental Science, Policy and Management, University of California Berkeley, Berkeley, California,

²Center for Accelerator Mass Spectrometry, Lawrence Livermore National Laboratory, Livermore, California,

³Physical and Life Sciences Directorate, Lawrence Livermore National Laboratory, Livermore, California, USA

Correspondence

Allegra C. Mayer, Department of Environmental Science, Policy and Management, University of California Berkeley, Berkeley, CA, USA. Email: mayer25@llnl.gov

Funding information

Office of Science, Grant/Award Number: SCW1572; National Institute of Food and Agriculture, Grant/Award Number: CA-B-ECO-7673-MS: National Science Foundation Division of Earth Sciences, Grant/Award Number: EAR-1331841 and EAR-2012878: Lawrence Graduate Research Scholarship, Lawrence Livermore National Laboratory: National Science Foundation Division of Environmental Biology, Grant/Award Number: DEB-1546686 and DEB-1831952

Abstract

Increasing hurricane frequency and intensity with climate change is likely to affect soil organic carbon (C) stocks in tropical forests. We examined the cycling of C between soil pools and with depth at the Luquillo Experimental Forest in Puerto Rico in soils over a 30-year period that spanned repeated hurricanes. We used a nonlinear matrix model of soil C pools and fluxes ("soilR") and constrained the parameters with soil and litter survey data. Soil chemistry and stable and radiocarbon isotopes were measured from three soil depths across a topographic gradient in 1988 and 2018. Our results suggest that pulses and subsequent reduction of inputs caused by severe hurricanes in 1989, 1998, and two in 2017 led to faster mean transit times of soil C in 0-10 cm and 35-60cm depths relative to a modeled control soil with constant inputs over the 30-year period. Between 1988 and 2018, the occluded C stock increased and δ¹³C in all pools decreased, while changes in particulate and mineral-associated C were undetectable. The differences between 1988 and 2018 suggest that hurricane disturbance results in a dilution of the occluded light C pool with an influx of young, debris-deposited C, and possible microbial scavenging of old and young C in the particulate and mineral-associated pools. These effects led to a younger total soil C pool with faster mean transit times. Our results suggest that the increasing frequency of intense hurricanes will speed up rates of C cycling in tropical forests, making soil C more sensitive to future tropical forest stressors.

KEYWORDS

¹⁴C, Hurricane Hugo, Hurricane Maria, Luquillo Experimental Forest, radiocarbon, soil carbon age, transit times

INTRODUCTION

Humid tropical forests have among the highest net primary productivity (NPP) globally (Running et al., 2004), as well as the fastest decomposition rates (Parton et al., 2007). High inputs coupled with rapid decomposition lead to globally significant fluxes of carbon (C) both into and out of tropical forest soil. Disturbances, such as extreme weather events, are important drivers of C inputs and losses from soils (Wu et al., 2011). Hurricanes are a regular disturbance in some tropical regions. Severe hurricanes (categories 3-5) have become more frequent (Kossin et al., 2020), and very severe hurricanes (categories 4 and 5) may become more frequent under future climate

Karis J. McFarlane and Whendee L. Silver are joint senior authors.

This is an open access article under the terms of the Creative Commons Attribution-NonCommercial-NoDerivs License, which permits use and distribution in any medium, provided the original work is properly cited, the use is non-commercial and no modifications or adaptations are made. © 2024 The Authors. Global Change Biology published by John Wiley & Sons Ltd.

change (Knutson et al., 2020). Understanding the fate of C produced in these ecosystems and how hurricanes affect net gains or losses of C over decadal timescales is key to accurately assessing future climate conditions.

Between 1989 and 2019, four major hurricanes have impacted the Luquillo Experimental Forest (LEF), Puerto Rico. The occurrence of four hurricanes over a 30-year period is more frequent than predicted by the long-term record of 60-year return intervals (Scatena & Larsen, 1991). The combination of increasing hurricane frequency accompanied by high litter inputs and fast decomposition rates (Ostertag et al., 2003) have contrasting and unquantified effects on soil C storage. The net C balance is strongly influenced by the residence time of C stabilized in soils, making the vulnerability of soil C to hurricane events an important and unresolved question.

The changes in forest structure and environmental conditions following severe hurricanes have competing effects on C stocks in tropical soils. First, soil C stocks could increase with the large pulse of plant debris associated with a hurricane (Beard et al., 2005; Liu, Zeng, Zou, Gonzalez, et al., 2018; Liu, Zeng, Zou, Lodge, et al., 2018; Scatena & Lugo, 1995; Scatena et al., 1993; Silver et al., 1996; Vogt et al., 1996). These inputs are primarily composed of young, recently fixed C. Simulated hurricane debris deposition has been shown to increase soil C concentrations at 50 cm depth 10 years after deposition, suggesting that the disturbance could increase C in subsurface soils over years to decades (Gutiérrez del Arroyo & Silver, 2018). Large pulses of recently derived "young" C from hurricane debris could also dilute the existing older soil C and decrease the mean age of the soil C pool while increasing total soil C concentrations.

Second, soil C stocks could decrease due to reduced inputs in the years following a severe hurricane. The open canopy and altered microclimatic conditions in the forest floor after hurricanes have been shown to reduce litter inputs above and belowground for at least 6 years after a hurricane (Beard et al., 2005; Silver et al., 1996; Vogt et al., 1996). A boom-bust cycle in the supply of new litter inputs could lead to a net loss of soil C stocks as microbial consumption shifts towards increased use of pre-existing (older) soil C in the years of low litter inputs prior to full recovery (Guenet et al., 2012; Kuzyakov et al., 2000; Sayer et al., 2007). During the prolonged period of reduced inputs, microbial scavenging could consume and respire both modern and older C, leaving the soil C pool more depleted in radiocarbon and the mean soil age potentially older until a major pulse of young, modern litter inputs are deposited during the next hurricane. Increased loss of older soil C during the recovery period may be compounded over multiple severe hurricane events. In the tropics, reduced C inputs to soil associated with frequent hurricane events may mirror the effects of land use change, particularly deforestation, which also results in decreased C inputs to soil, decreased soil C pools, and older soil C ages (Finstad et al., 2020; Nagy et al., 2018; Trumbore et al., 1995).

In this study, we compared soils sampled more than 50 years after any major hurricane with soil from the same sites after four major hurricanes over a 30-year period to examine how more frequent hurricanes influence age (time since C has entered the pool),

transit time (time between entry and exit from the bulk soil; Sierra et al., 2017), and fluxes of C from particulate, aggregate-occluded, and mineral-associated pools in the soil surface and subsurface. We used the rapidly changing atmospheric concentrations of ¹⁴C between the two sampling dates to constrain model simulations to numerically determine the distribution of annual to centuries-old soil C ages and cycling rates. We tested the hypothesis that multiple years-long reductions of litter inputs (such as the reductions that occur following severe hurricanes) would decrease overall soil C stocks and increase the mean age of both mineral-associated and particulate soil C.

2 | METHODS

2.1 | Site description

Soils were sampled from the Bisley Experimental Watershed (henceforth Bisley) of the LEF, Puerto Rico (18.3157 N, 65.7487 W), a Long-Term Ecological Research and Critical Zone Observatory and Network site (https://luq.lter.network). The mean daily temperature at Bisley was approximately 24°C between 1993 and 2003 (González, 2015), and 23.7°C between 2000 and 2016 (González, 2017), with little seasonality. Mean annual precipitation at Bisley was 3883 (\pm 864SD) mm y⁻¹ from 1988 through 2014 (González, 2017; Murphy et al., 2017), though drought conditions occurred in 2015, reducing precipitation input in the years preceding 2018 (Gonzalez, 2023). Rainfall occurs all year, though January through April experience slightly less precipitation than other months (Heartsill-Scalley et al., 2007). The site is a humid tropical forest with a diverse tree community of approximately 170 species >4cm diameter at breast height (Weaver & Murphy, 1990), and dominated by tabonuco (Dacryodes excelsa Vahl). The elevation of Bisley spans from approximately 260 m a.s.l. at the base to 450 m a.s.l. on the ridges (Scatena, 1989).

Soils in Bisley are derived from volcaniclastic sediments of andesitic parent material (Scatena, 1989). Ridge soils are classified as Ultisols (Typic Haplohumults), while slope soils are classified as Oxisols (inceptic and Aquic Hapludox), and valley soils are classified as Inceptisols (Typic Epiaquaepts) (Hall et al., 2015; McDowell et al., 2012; Scatena, 1989). Detailed site descriptions can be found in Scatena (1989), Heartsill-Scalley et al. (2010), and McDowell et al. (2012). Here we refer to soil organic C (SOC) and soil C interchangeably because there was no detectable inorganic C in these soils.

2.2 | Hurricane occurrence

Nine major hurricanes (category 3 or higher) have impacted Puerto Rico between 1851 and 2019 (López-Marrero et al., 2019), and five of these hurricanes have impacted the LEF. Until 1998, hurricanes had historically directly impacted the LEF approximately

FIGURE 1 Timeline of major hurricanes that have affected Luquillo Experimental Forest between sampling dates.

every 60 years (Scatena & Larsen, 1991). Prior to the initial sampling campaign of this study, Hurricane San Ciprián in 1932 was the most recent storm to cause major disturbance to the LEF (Scatena & Larsen, 1991). However, since sampling in 1988, four major hurricanes have impacted the forest through 2019 (Figure 1). Hurricane Hugo (Category 3) in 1989, Hurricane Georges (Category 3) in 1998, and Hurricanes Irma and Maria (Categories 5 and 4, respectively) within a 2-week period in 2017. The trajectory and wind speeds of all these hurricanes caused widespread defoliation. Litterfall following these defoliation events historically took over 5 years to return to pre-hurricane levels (Scatena et al., 1996).

2.3 | Sampling

Sample collection occurred in 1988 and again in 2018. In both years, samples were collected from three depths: 0–10cm (the A horizon), 10–35cm (all of the B1 horizon and part of B2), and 35–60cm (B2 to C) using an 8cm diameter soil auger. Soils in this study were sampled at three separate sites at least 40m from one another for each of the three topographic locations: ridge, slope, and upland valley. Two separate cores were taken from a fourth topographic location in the riparian valley that characterized a smaller proportion of the area of these watersheds (Scatena & Lugo, 1995). Riparian valley sites were ephemeral streambeds with a high boulder presence that limited sampling to less than 25cm depth in one case. Sampling sites from 1988 were marked with flags, and samples from 2018 were collected from within 15m of the same locations as the replicates from 1988, for consistency.

Samples collected in 1988 were analyzed for bulk density, pH, soil moisture, and a suite of soil chemical properties (see Silver et al., 1994). Samples were then air dried and stored in closed Ziploc bags within paper bags in a storage facility in Richmond, CA, USA, prior to density fractionation in 2018. Storage in plastic bags could potentially have contaminated the light fractions in these 1988 samples with very low fossil ^{14}C if degraded plastic had been present in the 1988 samples. However, highly enriched $\Delta^{14}\text{C}$ values in the 1988 light fractions indicate that the C present is dominated by bomb-derived ^{14}C , and no major plastic contamination occurred. Fresh samples collected in 2018 were also characterized for pH, soil moisture, and soil chemistry. Approximately 3g of subsamples from each fresh sample in 2018 were immediately extracted with 45 mL

of a 0.2M sodium citrate/0.5M ascorbate solution, shaken for 16h, then centrifuged and the supernatant decanted to measure concentrations of poorly crystalline iron (Fe) oxides. Within 2 days of being double-bagged in Ziploc bags, fresh samples were further subsampled and analyzed for pH in a 1:1 soil-to-water slurry (Thomas, 1996) and for gravimetric soil moisture by oven-drying ~10g of subsamples at 105°C until a constant weight was reached. Soil samples were air dried before further processing and analysis. Air-dried soils from both sampling years were sieved to 2 mm, and large roots were sorted out. We compared bulk density from our samples in 1988 to bulk density from a 2019 study sampling from the same forest and two of the same landscape positions (Ridge and Upland Valley) at 0-5 and 7-12 cm depths (Cabugao et al., 2021; Norby et al., 2019). We performed a Tukey's Honest Significant Difference test on an unpaired analysis of variance to compare the 1988 versus 2019 bulk density from the same landscape positions and similar depths. We found that bulk density values were similar and not statistically different between years, with 95% confidence intervals overlapping zero (p=.25). Thus, we use the same bulk density values in 1988 and 2018 for our calculations of SOC stock.

2.4 | Soil density fractionation

Soil C can be separated conceptually and operationally into three pools, each cycling at a different mean rate. Particulate C is generally composed of the youngest C, with aggregate-occluded C intermediate-aged and mineral-associated C the oldest SOC (Schrumpf et al., 2013; Sollins et al., 2009). Mineral-associated C has mean turnover times ranging from decades to millenia, indicating a higher average degree of stability (McFarlane et al., 2013; Trumbore et al., 1995). Soils were fractionated by density following the method of Swanston et al. (2005), as modified by Marin-Spiotta et al. (2009). Approximately 20g of air-dried soil was added to centrifuge tubes. Sodium polytungstate (SPT, Na6 [H2W12O40] TC-Tungsten Compounds, Bavaria, Germany) in a solution of density 1.85 g cm⁻³ was added to centrifuge tubes and agitated before centrifuging. The density of the SPT followed previous studies from this and nearby sites to allow direct comparison (Gutiérrez del Arroyo & Silver, 2018; Hall et al., 2015). Particulate organic matter floating at the surface after centrifugation, the free light fraction (FLF), was aspirated and then rinsed with 100 mL of deionized water five times on a 0.8 µm pore polycarbonate filter (Whatman Nuclepore Track-Etch Membrane, Darmstadt, Germany). Rinsed FLF was oven dried at 65°C until the weight had stabilized. The remainder of the sample was combined with 70 mL of additional SPT and mixed using an electric benchtop mixer (G3U05R, Lightning, New York, NY, USA) at 1700rpm for 1min and sonicated in an ice bath for 3min at 70% pulse (Branson 450 Sonifier, Danbury, CT, USA). Sonication is intended to disrupt soil structure and liberate organic matter that had been occluded in aggregates. The sonicated slurry was centrifuged again, and the light fraction at the surface, the occluded light fraction (OLF), was aspirated, rinsed, and dried using the same

3652486, 2024, 4, Downloaded from https://onlinelibrary.wiley.com/doi/10.1111/gcb.17265, Wiley Online Library on [12/06/2024]. See the Terms and Conditions (https://onlinelibrary.wiley.com/terms-and-conditions) on Wiley Online Library for rules of use; OA articles are governed by the applicable Creative Commons Licenses

method as for the FLF. The remaining soil pellet was considered the heavy fraction (HF), or mineral-associated organic matter fraction, which encompassed all mineral sizes, including sand. The HF was rinsed by thoroughly mixing with 150 mL of deionized water in the centrifuge tube, centrifuging, and removing the supernatant repeatedly until the fraction had been rinsed five times. The rinsed HF was oven dried at 105°C until the weight stabilized. The average mass recovery was 98%.

Soil C and N and δ^{13} C 2.5

Dried bulk and HF soils were homogenized separately using a Spex Ball mill (SPEX Sample Prep Mixer Mill 8000D, Metuchen, NJ). The FLF and OLF were homogenized separately by hand using a mortar and pestle. All homogenized samples were then analyzed at U. C. Berkeley for C and N concentrations on the CE Elantech elemental analyzer (Lakewood, NJ) and for δ^{13} C in the Stable Isotope Laboratory at UC Berkeley, using a CHNOS Elemental Analyzer interfaced to an IsoPrime 100 mass spectrometer (Cheadle Hulme, UK), with a long-term external precision of 0.10%. Soil C stocks were calculated by multiplying the C concentrations (%) by the oven-dry mass of bulk soil (<2 mm) and dividing by depth and the bulk density as measured in 1988 (Silver et al., 1994; Throop et al., 2012). Bulk density measurements from 6 months after samples were taken in 2018 from the same forest and topographic positions were not statistically different from bulk density in 1988 (p=.25; 95%) confidence intervals overlapping zero; Cabugao et al., 2021; Norby et al., 2019).

2.6 Radiocarbon

Homogenized soil samples were combusted to CO2 in sealed glass tubes along with silver (Ag) and copper oxide (CuO) at the Center for Accelerator Mass Spectrometry at Lawrence Livermore National Lab. The CO₂ was then graphitized on Fe powder under pressurized hydrogen gas (Vogel et al., 1984). Graphite was pressed into aluminum targets and run on the Compact Accelerator Mass Spectrometer for radiocarbon analysis (Broek et al., 2021). Radiocarbon is reported in Δ^{14} C, following Stuiver and Polach (1977), and calculated based on the fraction of modern isotope composition, corrected for the year of sampling, and corrected for mass-dependent fractionation with observed $\delta^{13}C$ values of the sample. The compact AMS had an average Δ^{14} C precision of 3.2%. We report the corrected Δ^{14} C value and $\Delta\Delta^{14}$ C, which is calculated as Δ^{14} C of the sample minus Δ^{14} C of the atmosphere, to account for rapidly changing atmospheric Δ^{14} C during the study period. Atmospheric radiocarbon has been decaying nonlinearly since the peak of weapons testing in the 1950s. Radiocarbon signatures in the soil are strongly influenced by the atmospheric Δ^{14} C signature, making them useful for modeling soil C age and transit time, especially since the 1950s. To compare the contribution of modern C between 1988 and 2018, it is useful

to take the difference between soil and atmospheric Δ^{14} C values, or $\Delta\Delta^{14}$ C, because atmospheric Δ^{14} C declined between 1988 (98%) and 2018 (4.4%) in Northern Hemisphere Zone 2 (Hua et al., 2013). We note that the decline in atmospheric Δ^{14} C is nonlinear, and thus the $\Delta\Delta^{14}$ C in 2018 soil will be less sensitive to short-term shifts in Δ^{14} C inputs than the samples from 1988.

Carbon age and transit time modeling

Transit times and ages of C were modeled with the package "SoilR" (Sierra et al., 2012, 2014) in R, version 4.0.2. The change in C density fractions over time, termed C flow, was modeled using a three-pool structure with a series flow matrix, under the simplifying assumption that C flows from the litter pool to the FLF, where it is sequentially transferred into the OLF and HF pools (Figure 2). We did a Markov chain Monte Carlo parameter optimization analysis on both a parallel flow model (inputs flowing each to FLF, OLF, and HF) and a series flow model (inputs flowing to FLF, then from FLF to OLF, and from OLF to HF), with the same input surface input assumptions and biological constraints. We found that a series model was a much better fit to the observed radiocarbon data of the OLF and HF pools than the parallel model, especially at the deeper depths. We present the outputs from a series model and acknowledge that the reality of C flow is likely some combination of the two flow pathways. The $\Delta\Delta^{14}$ C of the FLF in 1988, prior to the recent spate of hurricane events, was the most positive of the pools and was dominated by modern bomb C, while the HF pool $\Delta\Delta^{14}$ C was the most negative and dominated by pre-bomb C. This pattern suggests that C enters first into the FLF pool and is transferred over time into the

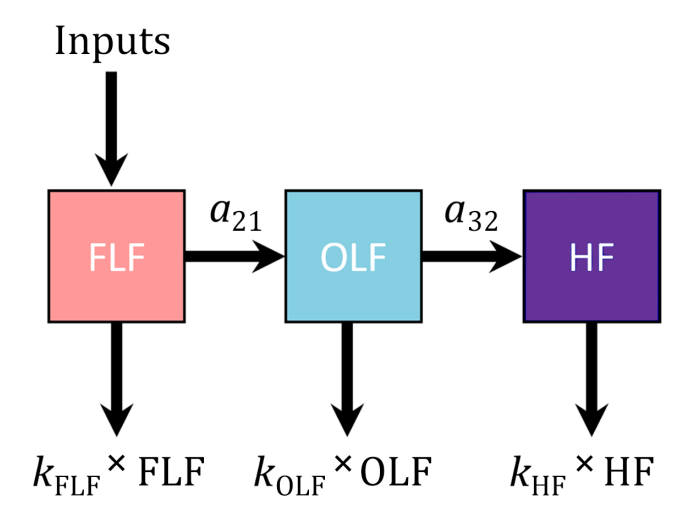


FIGURE 2 Hypothesized flow of C in soils for each depth. Free light fraction (FLF) C (pink) is either decomposed (at cycling rate $-k_{FIF} \times FLF$) or transferred to the occluded light fraction pool (OLF, blue) with the transfer proportion defined by a_{21} . Carbon transfer between the OLF and heavy fraction (HF, purple) is defined by transfer coefficient a_{32} , and is respired from these pools at cycling rates $-k_{\text{OLF}} \times \text{OLF}$ and $-k_{\text{HF}} \times \text{HF}$, respectively. Figure adapted from Sierra et al. (2012).

Model structure is depicted in basic form in Equation (1),

$$\frac{dC(t)}{dt} = Inputs - k \times C, \tag{1}$$

in matrix form with explicit pools in Equation (2),

$$\left(\frac{dC(t)}{dt}\right) = \begin{pmatrix} \text{Litter Inputs} \\ 0 \\ 0 \end{pmatrix} + \begin{pmatrix} -k_{\text{FLF}} & 0 & 0 \\ a_{21} & -k_{\text{OLF}} & 0 \\ 0 & a_{32} & -k_{\text{HF}} \end{pmatrix} \begin{pmatrix} C_{\text{FLF}} \\ C_{\text{OLF}} \\ C_{\text{HF}} \end{pmatrix}$$
(2)

where k is the first-order decay constant for each pool, a is the C transfer rate between pools (i.e., a_{21} is the transfer from FLF [pool 1] to OLF [pool 2] and a_{32} is the transfer from OLF [pool 2] to HF [pool 3]), and C is the C stock of each pool. The transitTime and systemAge functions within the "soilR" package use this model structure to solve for the distribution of ages (time since entry) of each pool, and the distribution of transit times (times between entry and exit from the bulk soil) (Sierra et al., 2018). Distributions of age and transit time were time-independent and do not assume a specific distribution (Sierra et al., 2014, 2017).

Soil Δ^{14} C and C stock means and SDs from each time point, depth, and fraction were used to constrain the matrix model describing movement of C through three soil pools and losses of C from each pool separately at each depth. Topography was not a strong predictor of patterns in Δ^{14} C, C stocks, or C fractions, so samples from all topographies were aggregated for model simulations. The model used the mean observed C content in each pool for each depth in 1988 as the initial condition for SOC stocks. Above and belowground litter inputs at 0-10cm were assumed to be 900g C m⁻² in non-hurricane or hurricane recovery years, based on observations from the same site (Liu, Zeng, Zou, Gonzalez, et al., 2018; Liu, Zeng, Zou, Lodge, et al., 2018; Scatena et al., 1996; Silver et al., 1996; Vogt et al., 1996).

Inputs to the 10-35cm and 35-60cm depths were estimated using observations of live fine roots in the surface and typical root distribution in the forest (Silver & Vogt, 1993). Total root input is approximately threefold the input of fine roots alone (McCormack et al., 2015; Yaffar & Norby, 2020), and live fine roots in the 0-10cm depth had a mean biomass of 80-250g C m⁻² (Hall et al., 2015), suggesting that total root C inputs of approximately 450 g C m⁻² to the surface would be well within the expected range. Root inputs below 0-10cm were estimated assuming that inputs follow the typical distribution of root biomass in Puerto Rican tropical forests, with 60%-70% of root biomass is in 0-10cm, an additional 20%-30% of biomass is in 10-35cm $(\sim 135 \,\mathrm{g}\,\mathrm{C}\,\mathrm{m}^{-2})$, and 5%–8% of biomass is in the 35–60 cm depth ($\sim 40 \,\mathrm{g}$ C m⁻²; Silver & Vogt, 1993; Yaffar & Norby, 2020).

The model was parameterized under two scenarios for each depth: (1) constant inputs, assuming a steady-state undisturbed forest; and (2) hurricane inputs, which simulated the input fluxes from defoliation during the four major hurricanes, followed by a subsequent reduction in litter inputs and then litterfall increasing linearly to pre-hurricane inputs over 6 years (Scatena et al., 1996;

Silver et al., 1996; Vogt et al., 1996). Hurricane inputs were imposed as an additional pulse of litter inputs at each depth interval, declining with depth. The 0-10cm interval received 100% of the surface input pulse, the 10-35 cm depth received a pulse of root inputs equivalent to 30% of the surface input pulse, and the 35-60 cm depth received root inputs equal to 10% of the surface input pulse, approximating observations following Hurricane Maria (Yaffar et al., 2021). Surface litter pulses under hurricanes were specified according to measured litterfall values and were 42.5 g C m⁻² to the surface in 1989 (Hurricane Hugo) and 1998 (Hurricane Georges; Scatena et al., 1993; Silver et al., 1996) and 1611 g C m⁻² in 2017 (Hurricanes Irma and Maria; Liu, Zeng, Zou, Gonzalez, et al., 2018). The same soil Δ^{14} C and C stock observations were used to constrain the model under each scenario, with only the input regime varying.

Parameters of the transfer matrix $(-k_{\text{FLF}}, -k_{\text{OLF}}, -k_{\text{HF}}, a_{21}, a_{32})$ were constrained using a cost function to accept or reject potential parameter sets over 1000 iterations, based on observed $\Delta^{14}C$ and C stock means and standard errors from both time points (1988 and 2018). A Markov chain Monte Carlo (MCMC) simulation initialized with cost-optimized parameters was run to assimilate observed data and optimize parameter choices to the observations using function modMCMC() from R package "FME" (Sierra et al., 2014; Soetaert & Petzoldt, 2010). The MCMC was iterated over at least 20,000 simulations or until parameter solutions converged according to the trace, which was over 100,000 iterations at the 35-60cm depth. The first half of the iterations were considered the burn-in period before the chain starts to converge near an equilibrium, and these iterations were discarded in calculations of optimal parameters. A list of optimal parameters can be found in Table S4. The model output for the surface soils of the HF pool was validated using published radiocarbon values from the mineral-associated fraction (the only fraction analyzed) of samples from the site taken in 2012 (Hall et al., 2015).

Bulk and pool soil C age and transit time density distributions and mean values were calculated using the systemAge() and transit-Time() functions from the "SoilR" package. Mean density distributions were calculated using the mean parameter set given from the MCMC analysis. The standard deviation from the mean was calculated using the systemAge() and transitTime() functions on 200 sets of five parameters selected randomly within one standard deviation of the mean of each parameter given as output from the MCMC. The lower and upper limits of SOC ages and transit times were calculated using the upper and lower ranges of these iterations.

2.8 **Statistics**

Statistics were run in R, version 4.0.2 (R Core Team, 2020). The statistical model selection followed the recommendations of Zuur et al. (2009). Statistical models were chosen using a linear mixed effects model in package "Ime4", with random slopes accounting for the influence each core, or sampling site, had on the response variable values as it varied with depth. This random effect of the core site on the depth effect was evaluated using a restricted maximum likelihood approach and was included in the initial evaluation of all model comparisons. Linear mixed effect models included year, topographic position, depth, and interactions as fixed factors, and the depth effect of each core as a random factor for each of the response variables: C concentration, N concentration, δ^{13} C, $\Delta\Delta^{14}$ C. In evaluations of some response variables with the AIC and BIC criteria, the random effect no longer enhanced the model, and model comparison proceeded using ANOVAs of linear models without random effects. Topographic effects on C concentrations are discussed in the supplemental information. Model assumptions were evaluated using the check_model function in R package "performance" to check for multicollinearity, normality of residuals, homoscedasticity, homogeneity of variance, influential observations, and normality of random effects. Linear model outputs can be found in Table S2.

In cases where random effects were significant (bulk soil δ^{13} C and $\Delta\Delta^{14}$ C. FLF $\Delta\Delta^{14}$ C and HF C and N concentrations), fixed effects were chosen using ANOVA of subsequent models using maximum likelihood estimation, with the random effects held constant. Once fixed effects were established, the model was re-fitted using a restricted maximum likelihood approach to report model estimates, and an ANOVA was run to determine the significance of the response variable. In all cases, p-values were estimated using Tukey's honest significant post-hoc test to assess significant differences between variables in the package "agricolae" in R, and contrasts and standard errors of contrasts were estimated using the Ismeans() function in the package "Ismeans" in R. Values of p < .10 were reported as significant unless otherwise specified. Topographic position was not a significant predictor for most variables, so results are reported as means aggregated across positions.

RESULTS

Patterns in soil C over time

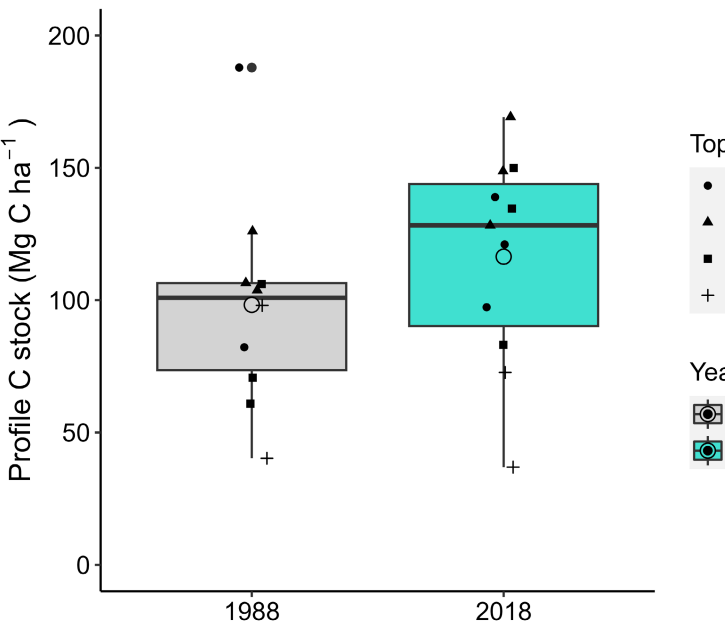
Soil C stocks in the 60 cm profile

Total soil C stocks summed from 0 to 60 cm did not vary significantly between years in the bulk soil (Figure 3, 1988: $98.2 \pm 12.7 \,\mathrm{Mg}$ C ha⁻¹ and 2018: $116.4 \pm 12.0 \,\mathrm{Mg} \,\mathrm{C} \,\mathrm{ha}^{-1}$, p = .2) or FLF, but did vary between years in the OLF (Figure 4). The mean OLF C increased by $7.7 \pm 3.8 \,\mathrm{Mg}$ C ha⁻¹ (p = .05) between sampling dates, from 8.6 ± 1.5 Mg C ha⁻¹ in 1988 to $16.4 \pm 3.5 \,\mathrm{Mg}$ C ha⁻¹ in 2018 (Figure 4). The mean total C stock in the HF was not statistically different (p=.3) between 1988 $(70.5 \pm 10.3 \,\mathrm{Mg}\,\mathrm{C}\,\mathrm{ha}^{-1})$ and 2018 $(84.9 \pm 10.3 \,\mathrm{Mg}\,\mathrm{C}\,\mathrm{ha}^{-1})$ when taken across topographic locations.

The proportion of C in the surface 0-10cm OLF increased from $16 \pm 7\%$ in 1988 to $21 \pm 6\%$ in 2018 (p < .05; Figure 5). The majority of soil C in this system was stored in the mineral-associated fraction (HF), increasing with depth from $58 \pm 11\%$ of C at 0-10 cm to $86 \pm 9\%$ of C at 35-60 cm (p < .001).

Patterns in stable C isotopes

Mean bulk soil δ^{13} C was more depleted in 2018 relative to 1988 by $2.2 \pm 0.3\%$ at 0-10 cm (p < .01) and by $1.4 \pm 0.3\%$ at 10-35 cm (p < .05), with no significant difference at the 35-60cm depth (Figure 6, Table 1). For each sampling time, mean δ^{13} C was significantly enriched in the $10-35 \,\mathrm{cm}$ ($+0.9 \pm 0.3\%$; p < .1) and 35-60 cm depths (+1.7 \pm 0.4%; p < .01) relative to the 0-10 cm depth in 2018, while there were no detectable differences with depth in 1988.



Year

Topo

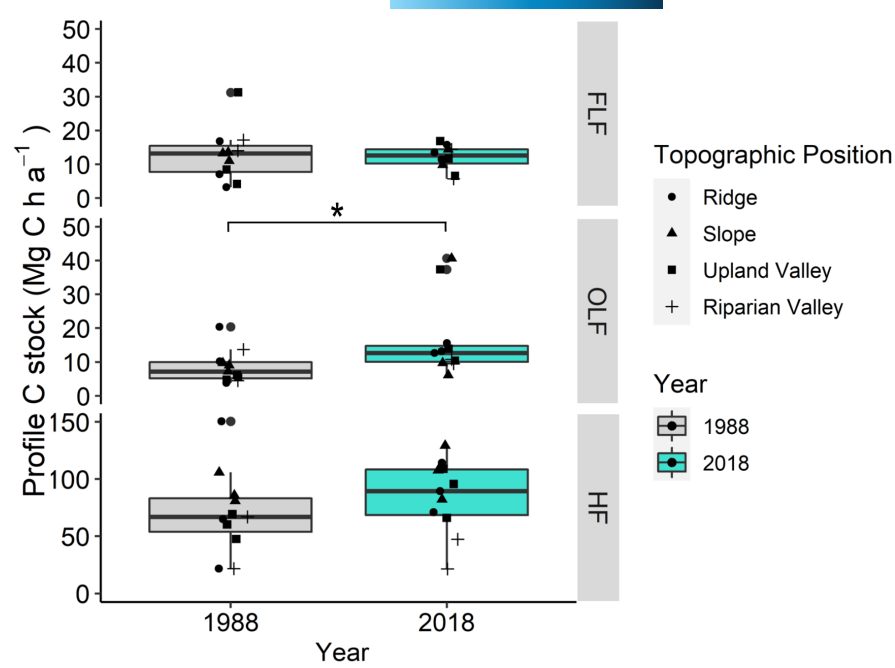
- Ridge
- Slope
- **Upland Valley**
- Riparian Valley

Year

- 1988
- **1** 2018

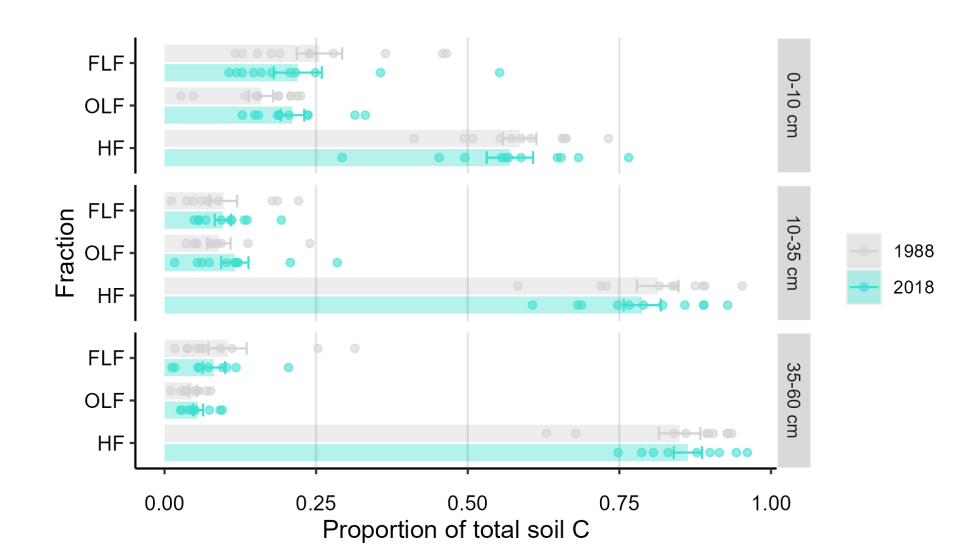
FIGURE 3 Soil C stocks (0-60 cm depth). The shape of each point indicates the topographic position of the soil core. The open circle is the mean value of whole-profile C stock, the thicker horizontal line of the summary boxplots is the median value, and the upper and lower borders of the box are the 25th and 75th quartiles for samples from 1988 (gray) and 2018 (turquoise).

FIGURE 4 Soil C stocks (0-60 cm depth) of density fractions calculated through mass balance. Black points represent individual profiles for the FLF (upper), OLF (middle), and HF (lower). Note the different scale for the v-axis of the HF figure. The shape of each point indicates the topographic position of the soil core. The thicker horizontal line of the boxes is the median value; the upper and lower borders of the box are the 25th and 75th quartiles for samples from 1988 (gray) and 2018 (turquoise). The asterisk indicates a statistical difference between whole-profile C stocks in each year (p = .05).



Global Change Biology

FIGURE 5 Mean proportion of total soil C (FLF+OLF+HF) for each fraction and depth (y-axis) in the years 1988 (gray) and 2018 (turquoise). Error bars indicate standard error (n = 11, except at 35-60 cm where n = 10).



Free light $\delta^{13}C$ decreased from 1988 to 2018 by $0.81 \pm 0.27\%$ in the 0-10 cm depth (p < .1). The mean OLF δ^{13} C signature decreased by $0.76 \pm 0.20\%$ at 0-10 cm (p<.01) from 1988 to 2018, and by $0.52 \pm 0.15\%$ at 10-35 cm (p < .01) and did not change detectably at 35-60 cm (Table 1). Surface (0-10 cm) soils in 2018 were significantly more depleted with respect to the $10-35 \,\mathrm{cm} \,(-0.45 \pm 0.15\%; \, p < .1)$ and 35-60 cm depths ($-0.85 \pm 0.17\%$; p < .01). There were no significant differences by topography between years.

Mean HF $\delta^{13} C$ signatures were significantly lower in the 0–35 cm depths in 2018 relative to 1988, decreasing by 0.97±0.22‰ at 0-10 cm (p < .01) and $0.87 \pm 0.13\%$ at 10-35 cm (p < .001) relative to 1988. The mean HF δ^{13} C became significantly more enriched between the 0-10 and 10-35 cm depths in 1988 (p < .05) and increased significantly with depth in 2018 (p<.05). Pooled means of HF δ^{13} C had a significantly more depleted signature than OLF and FLF δ^{13} C, which were not significantly distinct from one another.

3.1.3 | Patterns in radiocarbon

The difference in Δ^{14} C between sample and atmosphere ($\Delta\Delta^{14}$ C) in bulk soil decreased between 1988 and 2018 by $64 \pm 18\%$ in the 0-10 cm depth cm (p < .05; Figure S1). Bulk $\Delta \Delta^{14}$ C decreased significantly with depth at both time points (Table 1; p < .001 in all cases). The FLF $\Delta\Delta^{14}$ C decreased between 1988 and 2018, with the magnitude of decrease in 2018 varying with depth (Figure 7). The FLF $\Delta\Delta^{14}$ C decreased between 1988 and 2018 in the 0-10 cm (-73 \pm 12%; p < .001), 10-35 cm (-44 \pm 17%; p < .05), and 35-60 cm (-143 \pm 56%; p < .05) depths. The random variability of individual sample core with respect to depth was important, with core accounting for 90% of variance, of which 89% was a result of variability in the 35-60 cm depth. The mean occluded light $\Delta\Delta^{14}$ C was significantly reduced in 2018 relative to 1988 in the top 0–10 cm (–52 \pm 15%; p < .05). Occluded light $\Delta\Delta^{14}$ C decreased

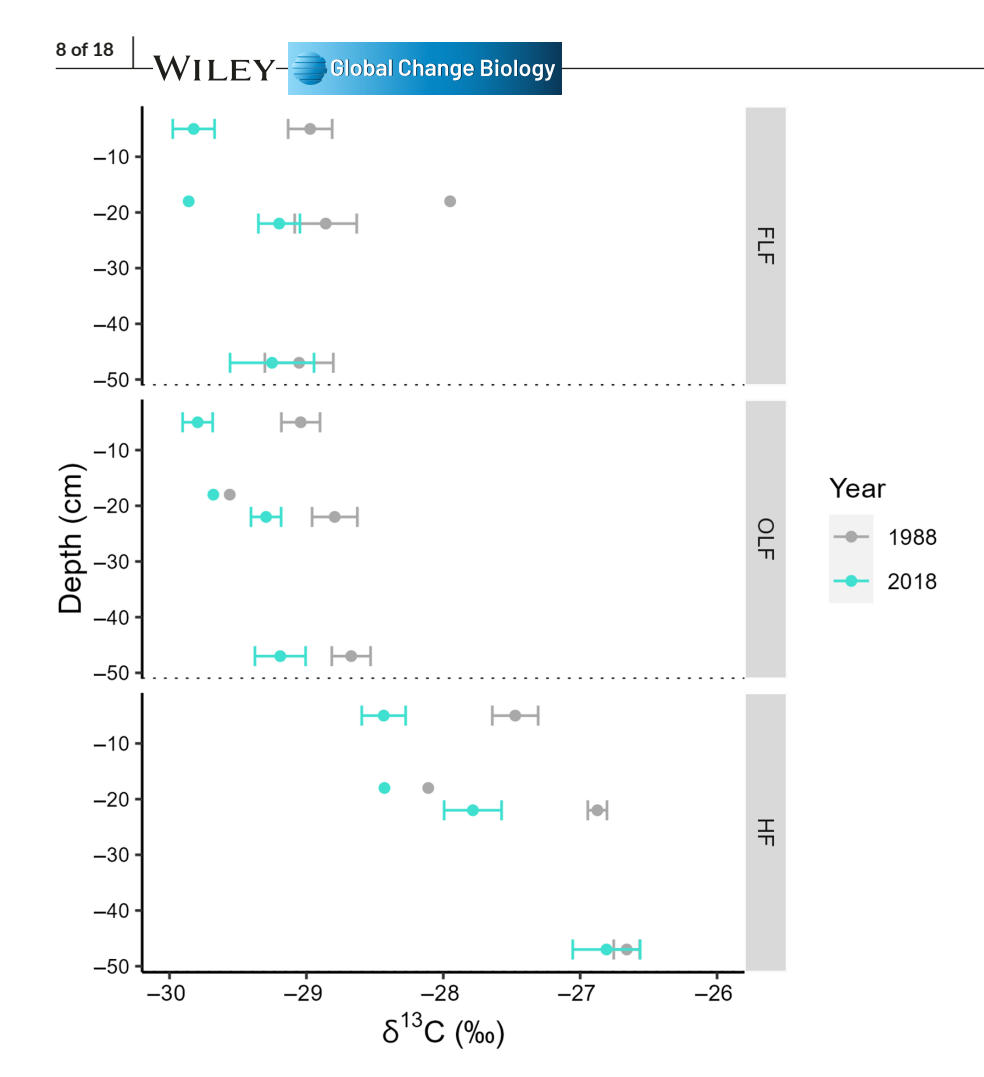


FIGURE 6 Mean δ^{13} C in % (x-axis) across all topographies (n=11, except at 35–60 cm where n=10) is plotted by depth from surface (y-axis) for soils sampled in 1988 (gray) and 2018 (turquoise). Free light fraction (upper), OLF (middle), and HF (lower) are plotted separately. Error bars indicate standard error and are included for every point except for the 10–25 cm depth from the riparian valley, which has only one replicate (Table S3).

significantly between 0 and 10 cm and the lower depths in 1988 (p < .001; Table 1).

The HF $\Delta\Delta^{14}$ C in 2018 increased significantly from 1988 values in the 10–35 cm (+116 \pm 32%; p<.01) and 35–60 cm depths (–138 \pm 49%; p<.05). In 2018, pooled mean HF $\Delta\Delta^{14}$ C in the 35–60 cm depth was significantly more depleted than the 0–10 cm depth (–212 \pm 33%; p<.001) and 10–35 cm depth (–169 \pm 47%; p<.05). In 1988, HF $\Delta\Delta^{14}$ C decreased significantly with each depth, by (–138 \pm 28%; p<.01) between 0–10 cm and 10–35 cm, and by (–172 \pm 48%; p<.05) between 10–35 cm and 35–60 cm. The mean $\Delta\Delta^{14}$ C for each fraction was lowest in HF.

3.1.4 | Hurricane effects of modeled soil C age and transit time distributions

Modeled bulk soil C age with constant inputs (control scenario) increased with depth from a mean of 39 years at 0–10 cm to 91 years at 10–35 cm and 153 years at 35–60 cm (Table 2). Mean bulk soil C age of hurricane-impacted soils (pulse of inputs followed by inputs that increased from zero to pre-hurricane levels linearly over 6 years, Figure 8) decreased by <1 year in the 0–10 cm depth, increased by 1 year in the 10–35 cm depth, and decreased by 20 years in the

35–60cm depth relative to soil with constant inputs. Optimized model parameters can be found in Table S4.

The modeled mean transit time under constant inputs was 9 years shorter than the mean bulk soil C age in the 0–10 cm depth, but 34 and 42 years greater than the mean bulk soil C age in the 10–35 cm and 35–60 cm depths, respectively (Figure 9a). Inclusion of hurricane-induced inputs to the model decreased mean bulk soil C transit time at all depths (Figure 9b). The hurricane scenario had the smallest effect on mean transit times in the 10–35 cm interval (–2 years) and the greatest effect in the 35–60 cm depth (–24 years). The mean bulk soil C age of the hurricane-impacted forest decreased in the 0–10 cm depth (–<1 year) and 35–60 cm depth (–20 years) relative to soil with constant inputs and increased (1 year) in the 10–35 cm depth.

Carbon pool ages increased from the FLF to OLF to HF at each depth in both the constant input and hurricane scenarios (Table 2, Figure 9c-e). For the scenario with constant inputs, the 0-10cm depth had mean pool ages of 1 (FLF), 3 (OLF), and 40years (HF). Despite the relatively similar mean pool ages, the distribution of ages within the pools differed. For example, 57% of FLF C was less than 1 year and all FLF C was younger than 10 years, while 30% of OLF C was less than 1 year and 98% of OLF C was younger than 10 years. Only 2% of HF C was younger than 1 year, and only 21% was younger than 10 years (Table 2).

TABLE 1 Mean (\pm SE; n=11, except at 35-60 cm where n=10) stable and radio-isotopic signatures by depth, year, and fraction. Asterisks indicate level of significance between years within fraction in each depth interval.

Depth interval	Year	Fraction	Mean δ^{13} C (‰)	SE	Mean Δ^{14} C (‰)	SE	Mean $\Delta\Delta^{14}$ C (‰)	SE
0-10 cm	1988	FLF	-29.0	0.2 [†]	207	12	109	12***
		OLF	-29.0	0.1**	208	15	110	15*
		HF	-27.5	0.2***	149	14	51	14
		Bulk	-26.8	0.3***	174	13	76	13*
	2018	FLF	-29.8	0.2 [†]	40	4	36	4***
		OLF	-29.8	0.1**	52	3	48	3*
		HF	-28.4	0.2***	53	3	49	3
		Bulk	-29.0	0.1***	47	3	12	3*
10-35 cm	1988	FLF	-28.9	0.2	193	17	95	17*
		OLF	-28.8	0.2**	105	22	7	22
		HF	-26.9	0.1***	-21	20	-119	20**
		Bulk	-25.6	0.1*	29	19	-69	19
	2018	FLF	-29.2	0.2	54	7	50	7*
		OLF	-29.3	0.1**	47	5	43	5
		HF	-27.8	0.2***	12	25	7	25**
		Bulk	-27.9	0.2*	23	10	-8	10
35-60 cm	1988	FLF	-28.9	1.0	216	64	118	64*
		OLF	-28.7	0.1	83	23	-15	23
		HF	-26.7	0.1	-154	31	-252	31*
		Bulk	-26.2	0.9	-75	25	-173	25
	2018	FLF	-29.0	0.9	-72	19	-76	19*
		OLF	-29.2	0.2	-7	12	-11	12
		HF	-26.8	0.2	-109	38	-114	38*
		Bulk	-26.9	0.2	-129	38	-160	36

^{***}p<.001; **p<.01; *p<.05;

The mean pool age of hurricane-impacted 0-10cm soil decreased by less than 1 year in the FLF and HF fractions and increased by 1 year in the OLF pool relative to the constant scenario. The proportion of C less than 1 year old changed by <1% in all three pools. The proportion of C less than 10 years old increased the slightly in the HF (21.8%-22.1%) due to hurricanes.

Hurricane inputs to the 10-35 cm depth decreased the pool age of FLF by 1 year (-25% change), decreased mean OLF age by 1 year (-1%), and increased mean HF age by 1 year. The probability distribution of C ages changed by <1% in the OLF and HF under hurricane inputs relative to constant inputs. The distribution of C less than 1 year since entry to the FLF increased from 21.5% to 26.5%, and the proportion of FLF C less than 10 years increased from 91.1% under constant inputs to 95.2% under hurricane inputs.

Imposing hurricane inputs rather than constant inputs reduced pool ages by the greatest amount in the 35-60cm in the OLF (-23 years) and HF (-20 years) pools. The change in the mean age of the FLF was negligible at this depth. Hurricanes also resulted in an increase in the proportion of C < 10 years old for the FLF (from 89.5% to 91.5%) and OLF pools (from 12.5% to 17.7%). At the 35-60 cm depth, hurricanes decreased the proportion of C that was >100 years

old by 47% in the OLF (from 25.8% to 13.8%), and by 11% in the HF pool (from 57.1% to 51.1%).

DISCUSSION

Changes in soil carbon stocks over time

Carbon stocks in the OLF increased between 1988 and 2018, along with the mean proportion of total C stored in the OLF pool. The lack of increase in the FLF pool, despite the recent pulse of litter inputs after Hurricanes Irma and Maria in 2017, suggests that environmental conditions caused by the opening of the forest canopy may have facilitated the rapid decomposition of hurricane-related fine litter debris (Gutiérrez del Arroyo & Silver, 2018; Ostertag et al., 2003). This same pulse in decomposition may help explain the enhanced quantity and proportion of C in the OLF pool, as the pulse of particulate organic matter may have provided the material and conditions for OLF formation. Occlusion of organic material in aggregates is most likely to occur following microbial decomposition to finer particles and the secretion of sticky exudates during microbial processing (Rabbi et al., 2020).

 $^{^{\}dagger}p$ < .1.

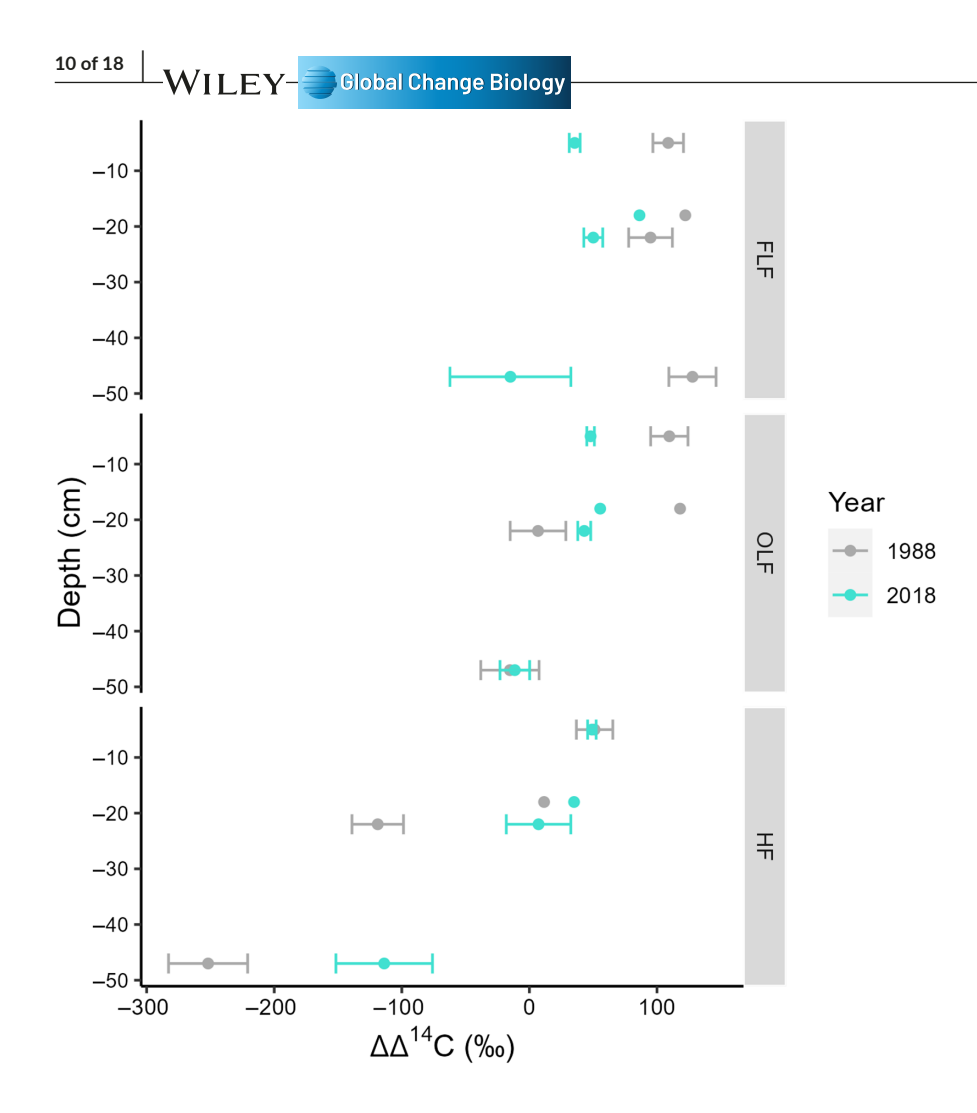


FIGURE 7 Mean change in radiocarbon ($\Delta\Delta^{14}$ C of sample minus atmosphere, x-axis) plotted throughout the depth profile (y-axis). Means of all topographic positions (n=11) are plotted for each depth for the years 1988 (gray) and 2018 (turquoise) and for the free light fraction (FLF, upper), occluded light fraction (OLF, middle), and heavy fraction (HF, lower). Error bars indicate the SE.

These results are consistent with the expected fingerprint of a recent hurricane: a boom in microbial activity responding to the pulse of hurricane-induced plant inputs.

4.2 | Patterns of δ^{13} C over time

Stable C isotope signatures decreased between 1988 and 2018 in the bulk soil and all three physical fractions. The decrease in δ^{13} C over time was most distinct in the 0-10cm depth and ranged from $0.76 \pm 0.20\%$ to $0.97 \pm 0.22\%$ across fractions. There are three possible explanations for the depletion of δ^{13} C over time. First, in the HF and OLF, an increase in the ratio of plant tissue C (more depleted in δ^{13} C) relative to more microbially processed C (more enriched in δ^{13} C) could have contributed to the overall depletion of the δ^{13} C signature over time. The FLF closely resembles plant material and is relatively unprocessed; thus, an increase in microbial processing is unlikely to explain a depletion of the magnitude observed in the FLF. A second possible explanation is an increase in the relative contribution of lignin-rich litter to the FLF, as lignin is up to 5% more depleted in δ^{13} C relative to other structural C components from the same plant (Fernandez et al., 2003). Lignin generally comprises a higher proportion of the total C in wood than in roots, and is higher in roots than in leaves (Fernandez et al., 2003; Zeikus, 1981). The

increased contribution of partially decomposed woody stems and branches with higher concentrations of residual lignin to SOC pools in the top 30cm in 2018 would be a reasonable explanation for a 0.7–1.0% decrease in the stable C isotope signature.

A third possible explanation is the rise in fossil-derived CO₂ from anthropogenic emissions, which depleted the atmospheric δ ¹³CO₂ that was subsequently fixed in the vegetation. This could particularly pertain to the negative shift in FLF δ^{13} C over time. The age distribution of FLF was approximately annual, implying that the δ^{13} C signature of the fast-cycling FLF would lag the decreasing atmospheric δ^{13} C by a few years at most, and be more enriched than the atmosphere. Carbon dioxide measurements since 1956 have exhibited a simultaneous increase in atmospheric \mbox{CO}_2 concentration and depletion of δ ¹³CO₂ due to the "Suess effect" (Keeling, 1979). The historic dataset from Mauna Loa, HI, USA recorded a -0.67% shift in δ^{13} C-CO₂ over the 30 years between 1984 and 2014 (Keeling et al., 2017). This atmospheric depletion is slightly smaller in magnitude than the -0.8% shift between 1988 and 2018 observed in the FLF in this study, implying that the Suess effect likely contributed to but was not the sole mechanism for the depletion observed in this study.

The depletion of $\delta^{13}\text{C}$ over time decreased with depth in the OLF, HF, and bulk soils, as $\delta^{13}\text{C}$ generally became more enriched with depth in the OLF in 2018 and in the HF in both sampling years. The enrichment of $\delta^{13}\text{C}$ with depth would be expected with

TABLE 2 Solutions of data assimilation-optimized three-pool model at each depth, as well as the system mean of all C pools (i.e., bulk soil C), with lower limits (LL) and upper limits (UL) as calculated using the SD of the second half of parameter sets from the Monte Carlo Markov Chain analysis.

0-10 900 Constant ELF 1 2 4 2 4 2 4 5 4 5 4 5 4 5 4 5 4 5 4 5 4 5 4 5 4 5 4 5 4 5 4 5 4 5 4 5 4 5 4 5 4 5 4 6 9	Depth (cm)	$Maxinputs(gCm^{-2})$	Inputs	Pool	Mean pool age (year)	ᆿ	ᅿ	Mean transit time (year)	ᆿ	Ы	%C age <1 year (%)	%C age <10 years (%)	%C age <100 years (%)
HF 40 26 89 2 2 88 2 23 885 885 885 885 885 885 885 885 885 88	0-10	006	Constant	FLF	1	1	2				56.6	100	100
Hericanes				OLF	က	2	4				30.5	98.5	6.66
900 Hurricanes FLF 1 2 6 30 21 58.6 100 105 2 3 3 4 5 6 60 98.6 100 135 Hr 40 2 3 2 4 2.4 5.4 5.2 100 98.6 100 98.6 100 100 98.6 100 98.6 100				生	40	26	88				2.3	21.8	91.9
900 Hurricanes FLF 1 1 2 3 6.6 100 135 Hr 40 27 55 3 24 22.1 135 Constant 11 40 27 5 4 5 24 22.1 135 Constant 11 4 4 4 5 4 5 4 5 135 LF 4 4 5 4 5 4 5 7 4 5 7 4 5 7 4 5 7 4 5 7 4 5 7 4 5 7 12 7 12 12 12 12 12 12 12 14 <t< td=""><td></td><td></td><td></td><td>Bulk</td><td>39</td><td>25</td><td>98</td><td>30</td><td>21</td><td>58</td><td></td><td></td><td></td></t<>				Bulk	39	25	98	30	21	58			
HF 40 2 39 3. 4 4. 4. 4. 4. 4. 4. 4. 4. 4. 4. 4. 4.	0-10	006	Hurricanes	FLF	1	1	2				56.6	100	100
HF 40 27 75 75 14 12 135				OLF	2	2	က				30.8	98.6	6.66
135 Constant FLF 4 5 4 5 4 6 4 6 4 6 4 6 4 6 4 6 4 6 7 6 7 12 7 11 135 Hr 92 37 1058 125 49 50.9 12.0 11.0 135 Hurricanes FLF 32 3 3 4 56.9 7 14.0 40 Hurricanes FLF 3 3 5152 123 3 12.0 12.0 12.0 40 Constant FLF 4 3 3 4 4 50.7 12.0 <td></td> <td></td> <td></td> <td>生</td> <td>40</td> <td>27</td> <td>75</td> <td></td> <td></td> <td></td> <td>2.4</td> <td>22.1</td> <td>91.8</td>				生	40	27	75				2.4	22.1	91.8
135 Constant FLF 4 4 5 4 5 4 5 4 4 5 44 4 12 12 115 115 116 116 12 116 <td></td> <td></td> <td></td> <td>Bulk</td> <td>39</td> <td>26</td> <td>74</td> <td>27</td> <td>20</td> <td>46</td> <td></td> <td></td> <td></td>				Bulk	39	26	74	27	20	46			
135 Hurricanes ELF 92 37 1058 49 5609 74 116 135 Hurricanes FLF 3 1058 40 5609 74 74 135 Hurricanes FLF 3 3 3 40 5609 75 74 40 Constant FLF 80 20 978 7 47449 73 11.6 40 Constant FLF 4 3 5152 123 37 147449 73 73 40 FLF 4 3 8 2 4 50.7 89.5 40 Hurricanes FLF 4 3 4 56.9 7 4 4 40 Hurricanes FLF 4 3 109 7 4 <td< td=""><td>10-35</td><td>135</td><td>Constant</td><td>FLF</td><td>4</td><td>4</td><td>5</td><td></td><td></td><td></td><td>21.5</td><td>91.1</td><td>100</td></td<>	10-35	135	Constant	FLF	4	4	5				21.5	91.1	100
HF 92 135				OLF	81	26	944				1.2	11.6	71.0
135 Hurricanes FLF 3 3 49 5609 26.1 95.2 135 Hurricanes FLF 3 3 3 1.2 26.1 95.2 40 Hr 93 31 5155 123 37 147,449 11.6 40 Constant FLF 4 3 8 2.1 47.7449 11.6 11.6 40 Constant FLF 4 3 8 4.7749 3 12.5 12.3 12.5 12.6				生	92	37	1058				0.7	7.4	65.5
135 Hurricanes ILF 3 3 3 3 3 4 55.2 4 55.2 4 55.2 12.2 12.2 12.5 11.6 40 Hr 93 31 515.5 123 37 147.449 7.3 7.3 40 Constant FLF 4 3 8 4.77449 7.3 7.3 7.3 40 Constant FLF 74 21 6089 7.2 7.4 7.3 7.3 7.3 40 Hurricanes FLF 156 68 42.759 194 84 567.399 4.4 4.4 40 Hurricanes FLF 4 3 10° 7 56.399 7.5 17.7 40 15 50 1090 7 2.18 9.15 7 5.0 7.5 9.5 7 7 9.5 9.5 9.5 9.5 9.5 9.5 9.5 9.5 9.5 9.5 9.5 9.5 9.5 9.5 9.5 9.5 9.5				Bulk	91	36	1005	125	49	2609			
40 OLF 80 20 978 1.2 1.2 1.6 40 Bulk 92 30 5152 123 37 147,449 7.3 40 Constant FLF 4 3 8 20.1 80.5 1.3 1.3 1.25 40 FLF 74 156 68 42,793 1.4 84 567,399 4.4 40 Hurricanes FLF 4 3 10 1.3 1.3 1.3 40 Hurricanes FLF 4 3 10 1.9 1.3 1.7 40 Hurricanes FLF 4 3 10 1.2 1.9 1.7 40 Hurricanes FLF 4 3 10 1.9 1.9 1.9 1.7 1.9 1.7 40 Hurricanes FLF 4 3 10,880 1.9 1.9 1.7 1.9 1.7 1.7 1.7 1.9 1.7 1.7 1.9 1.7 1.7 1.7 1.7	10-35	135	Hurricanes	FLF	е	က	ო				26.1	95.2	100
HF 93 31 5155				OLF	80	20	978				1.2	11.6	71.2
40 Constant FLF 4 3 6152 123 37 147,449 89.5 40 Constant FLF 4 21 6089 7 1.3 12.5 12.5 HF 156 68 42,759 194 84 567,399 4.4 40 Hurricanes FLF 4 3 10 21.8 91.5 40 Hurricanes FLF 50 20 1090 7 1.9 1.9 1.7 40 HF 135 58 10,880 7 6.5 5.0 5.0 80 10,885 17 70 36,808 5.0 5.0 5.0				生	93	31	5155				0.7	7.3	64.8
40 Constant ELF 4 3 8 8. 20.1 89.5 9.1 9.1 9.1 9.1 9.1 9.1 9.1 9.1 9.1 9.1				Bulk	92	30	5152	123	37	147,449			
40 156 689 1.3 1.3 12.5 HF 156 68 42,793 194 84 567,399 4.4 40 Hurricanes FLF 4 3 10 21.8 91.5 40 Hurricanes FLF 50 20 1090 1090 1.9 17.7 HF 135 58 10,880 7 6.5 5.0 Bulk 133 57 10,855 171 70 36,808 5.0	35-60	40	Constant	FLF	4	က	80				20.1	89.5	100
HF 156 68 42,793 74 64,759 44 567,399 4.4 40 Hurricanes FLF 4 3 109 75 75 178 179 170 170 170 170 170 170 170 170 170 170				OLF	74	21	6809				1.3	12.5	74.2
40 Hurricanes FLF 4 3 67 42,759 194 84 567,399 40 Hurricanes FLF 4 3 10 21.8 91.5 OLF 50 20 1090 1 1.9 17.7 HF 135 58 10,880 7 6.5 5.0 Bulk 133 57 10,855 171 70 36,808				生	156	89	42,793				0.4	4.4	42.9
40 Hurricanes FLF 4 3 10 21.8 91.5 OLF 50 20 1090 1.9 HF 135 58 10,880 0.5 5.0 Bulk 133 57 10,855 171 70 36,808				Bulk	153	29	42,759	194	84	567,399			
50 20 1090 1.9 17.7 135 58 10,880 0.5 5.0 133 57 10,855 171 70 36,808	35-60	40	Hurricanes	FLF	4	ო	10				21.8	91.5	100
135 58 10,880 0.5 5.0 133 57 10,855 171 70 36,808				OLF	50	20	1090				1.9	17.7	86.2
133 57 10,855 171 70				生	135	28	10,880				0.5	5.0	48.9
				Bulk	133	22	10,855	171	20	36,808			

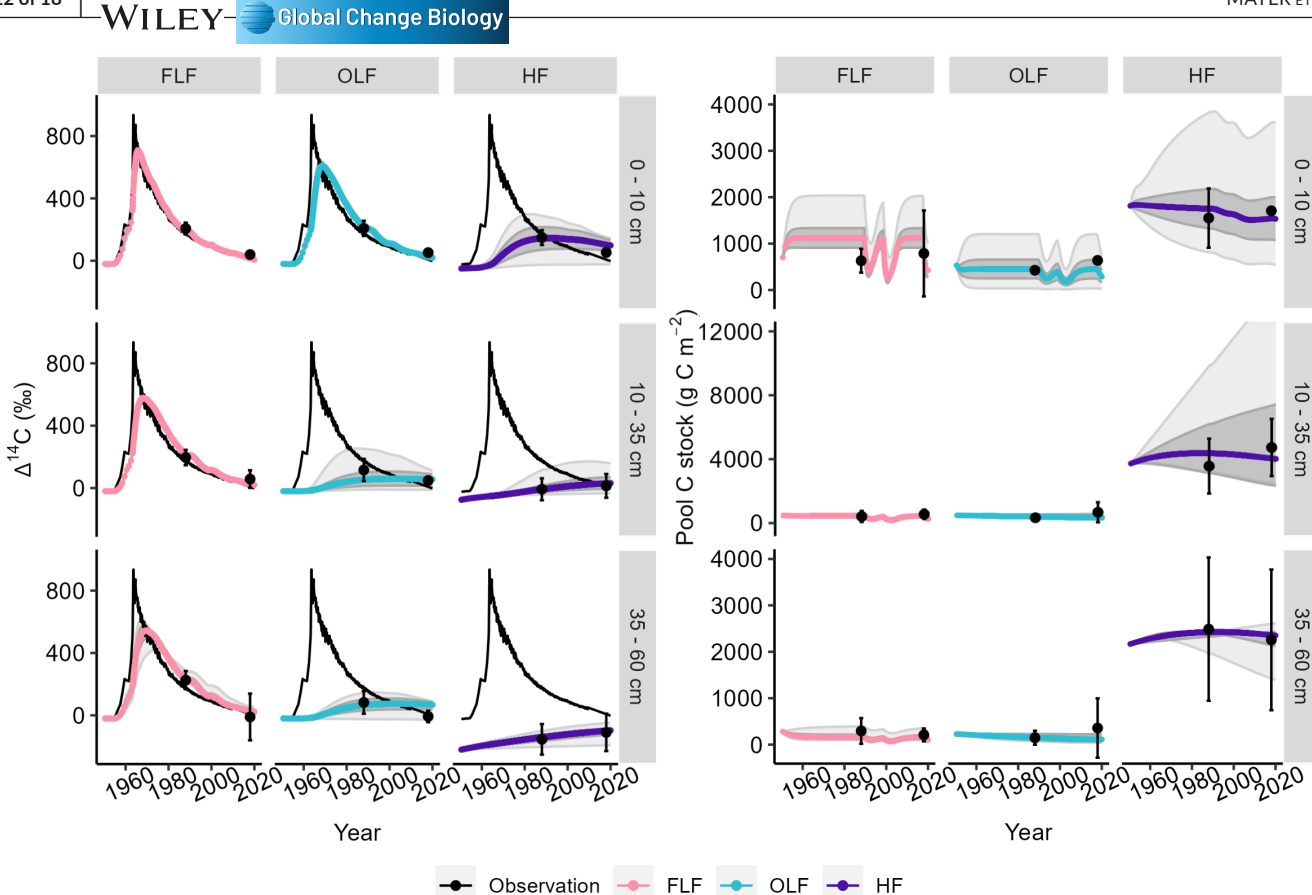


FIGURE 8 The mean and standard deviation (SD) of observed error (black points and error bars) are depicted for each fraction and depth. Mean SoilR model output is depicted for each depth and fraction (pink=FLF, turquoise=OLF, purple=HF), with SD (dark gray ribbon) and minimum and maximum (light gray ribbon) for possible parameter sets on at least 10,000 iterations. The left panel indicates radiocarbon signatures over time since 1950, with the black solid line showing atmospheric Δ^{14} C. The right panel shows the soil C stocks of each pool. All figures were simulated with hurricane inputs.

increased contributions of microbial C down the profile (Sollins et al., 2009). However, the increased depletion of 2018 $\delta^{13}C$ at the surface relative to the subsurface indicates an increased input of depleted $\delta^{13}C$ to the surface prior to that timepoint, consistent with any of the explanations listed above, and with the fingerprint of a pulse of plant material from recent hurricanes. However, the $\delta^{13}C$ depletion between 1988 and 2018 in the 0–35 cm depths of the HF, for which the C transit time distribution is dominated by C cycling on much longer than annual timescales (Trumbore, 2000), suggests hurricane influence from multiple hurricanes over decades.

4.3 | Patterns in Δ^{14} C over time

12 of 18

Radiocarbon in this tropical forest soil system was closely coupled to the change in atmospheric radiocarbon concentrations, suggesting rapid C cycling. In the 0–10cm depth, the 1988 FLF $\Delta^{14}\text{C}$ was +207% more enriched than values from the surface soil horizon of Oxisols in a Brazilian tropical forest in 1986 (+185%). The surface HF $\Delta^{14}\text{C}$ values were more depleted in the Brazilian study (Trumbore, 1993), indicating that there was a larger proportion of

quickly cycling soil C pool in this study than the soils in Brazil, and that in both cases, C cycled much more rapidly through all physical fractions than in temperate soils (McFarlane et al., 2013; Trumbore, 1993). Heavy fraction Δ^{14} C for the 0–10 cm depth was +27% more enriched in 2012 (Hall et al., 2015) than in 2018 for this site, which is the approximate rate of change in atmospheric Δ^{14} C in the 6-year period. Our results suggest that increased C inputs to mineral surfaces via frequent hurricane disturbance may result in faster cycling and transient mineral C (Neurath et al., 2021; Sayer et al., 2021).

Soil Δ^{14} C values are strongly influenced by the Δ^{14} C of litter inputs, which in turn depend on the Δ^{14} C of the atmosphere at the time of photosynthesis. To account for the effect of the 94% decrease in atmospheric Δ^{14} C between sampling dates in 1988 and 2018 (Hua et al., 2013), we must use the difference in soil Δ^{14} C from atmospheric Δ^{14} C ($\Delta\Delta^{14}$ C) to interpret the degree of incorporation of decadally cycling C in each fraction. In general, a positive $\Delta\Delta^{14}$ C signature indicates that the soil C was fixed within 30 years (in the case of 1988 soil) or 60 years (in the case of 2018 soil) because it contains more bomb C than the current atmosphere, with signatures closer to zero indicating a higher proportion of younger, recently photosynthesized C. In contrast, a negative $\Delta\Delta^{14}$ C signature

FIGURE 9 Mean probability density (y-axis) for the distribution of transit time (a), the mean time it takes C to exit the system, or age of C in each pool (b-e), the time since C entered the system in years (x-axis). Probability density functions are given at each depth under constant inputs (gray dashed line) or hurricane inputs (turquoise long dashed line). The gray and turquoise points at the top of the plot indicate the mean transit time (a) or mean C age (b-e) of the pool for each scenario, with error bars indicating the SD of the mean pool age (except where the upper limit of the SD is greater than 200 years and outside of the range plotted). Error bars that are not visible have a SD smaller than the width of the point. A subsample of 200 probability densities within the standard deviation of those simulated in the Monte Carlo Markov chain analysis is captured in the envelopes of the turquoise ribbon (hurricane inputs) and gray ribbon (constant inputs).

contains less bomb C than the current atmosphere and must therefore be dominated by pre-bomb, older C (fixed before ~1960). A negative signature that shifts closer to zero suggests increased

incorporation of bomb C. Heavy fraction $\Delta\Delta^{14}C$ did not change over time in the surface soil, but increased over time in the lower depths, with HF-associated C more enriched in $\Delta^{14}C$ in 2018 relative

to 1988. Because a greater proportion of the HF at depth cycles on longer timescales than the other two fractions, the increasing (but still negative) $\Delta\Delta^{14}$ C signature in 2018 relative to 1988 could reflect a ~30-60 year lag in the input of enriched bomb C to the system. Such a lag would mean that enriched bomb-derived Δ^{14} C would not yet be present in the 35 or 60 cm depth of the HF fraction in 1988, after only 30 years of enriched atmospheric Δ^{14} C, but in 2018, after 60 years of atmospheric enrichment, bomb-derived Δ^{14} C would be incorporated into the HF. The shift toward zero of the HF below 10cm depth is also consistent with the expected fingerprint of a regime of severe hurricanes, with repeated large depositions of modern C to the surface where it could cycle down the profile and shift $\Delta\Delta^{14}$ C closer to zero. The large shift in the lower 35-60 cm is unlikely to have resulted from a single hurricane (especially given that OLF $\Delta\Delta^{14}$ C did not shift at this depth), but rather a longer term, more consistent shift in inputs, either from a changing atmospheric Δ^{14} C, a shifting input regime due to frequent severe hurricanes, or a combination of the two.

4.4 | Simulated hurricane impacts on the soil system

Simulated hurricane-induced pulses followed by a 6-year recovery period of litter inputs resulted in younger mean bulk soil ages at depth and shorter mean transit times at most depth intervals. The mean age of C is a measure of time elapsed since C has entered the pool of interest, taken as a mean of the distribution of probable C ages (Sierra et al., 2017). The mean age of a pool can be misleading if the pool contains even a small proportion of very old C that can skew mean values to appear older than the majority of the soil matrix. A decrease in mean bulk soil age due to hurricanes could be driven by two mechanisms. First, a decrease in mean bulk soil age may result from the large flux of modern C deposited by each of the three hurricanes, diluting total C with young C and skewing the mean age younger. Alternatively, the decrease may result from increased microbial respiration of stabilized C. A short pulse of inputs could stimulate the decomposition of older C, leading to an overall younger soil C age, and potentially also a decline in the stabilized soil C stock. Carbon stocks did not decrease in any of the measured soil C pools in this study, suggesting that the inputs of new C to the mineral stabilized C pool were at least as great as the loss of older stabilized C.

The mean transit time is the average time it takes for C to leave the soil, weighted by input fluxes (Sierra et al., 2017). A decrease in mean transit time implies a greater proportion of C cycling quickly out of the pool. Evidence of a dilution effect would be an increase in C cycling rates following the hurricanes (sensu Ostertag et al., 2003) and increased C stocks, as well as an influx of new litter from storms. Decreased transit times could also indicate a more rapid efflux of older soil C. In this case, the increase in young C to total soil C stocks could be offset with the loss of older C, which could help explain the lack of significant changes to the HF

C stocks despite faster transit times in the HF pool. In this study, bulk soil transit time was most sensitive to changes in the HF, because mean transit time is most sensitive to changes in the pool with the slowest decomposition coefficient (Manzoni et al., 2009; Table S4). A laboratory incubation of soils from the same forest found significantly higher decomposition rates from soils sampled from a hurricane simulation plot relative to control soils (Liu, Zeng, Zou, Gonzalez, et al., 2018; Liu, Zeng, Zou, Lodge, et al., 2018), consistent with the faster transit time of C observed in this study. The observed faster transit times of the bulk soil (which is dominated by the HF) at all depths, and the younger mean ages in the 35-60 cm depth of the HF, which is often assumed to cycle more slowly than soils near the surface, are consistent with a shift in the input regime due to more frequent severe hurricanes. Together, the faster transit times without a significant increase in C stock suggest an increased loss of century-old mineral-associated soil C in a regime of increased severe hurricanes. A shift to more rapid cycling of soil C may result in more extreme soil C responses to forest stressors (e.g., tree mortality or canopy losses) that might reduce forest inputs in a changing climate. In this case, inputs might fail to keep pace with outputs over multiple years, which would result in a net loss of C from tropical soils, the recovery from which is unclear.

The impact of hurricanes on bulk soil C in the 0–10 cm depth was driven by the reduction in transit time and a shift in the age distribution of C in the heavy fraction. While the mean pool ages of FLF, OLF, and HF decreased by a year or less in hurricane simulation scenarios, the age *distribution* of C also shifted younger in these fractions (Figure 9).

The 0–10 cm depth was the initial repository of inputs from the hurricanes. Hurricanes had the largest impact on C age distribution and transit time as a proportion of initial mean ages in this depth. However, C also cycled very quickly in the constant input scenario (22% of HF less than 10 years old and 92% less than 100 years old), thus the absolute change in C age between the two scenarios was small. The mean ages of the soil C fractions were similar to previous calculations of steady-state mean residence time in 0–10 cm soil from nearby sites, as calculated using stable isotopes (Marin-Spiotta et al., 2009) and radiocarbon (Hall et al., 2015).

Carbon age distribution in the 35–60 cm depth was the most sensitive to simulated hurricane inputs of the depths studied. The mean C age of the OLF and HF C fractions each decreased by approximately 20 years under the hurricane scenario, due to a 12% and 6% respective decrease in the proportion of C greater than 100 years, as well as a 5% decrease in OLF C younger than 10 years old. Both changes could be explained by either a scavenging of older C leading to greater respiration of 100+ year-old C in the OLF and HF, or by significantly increased input of C between 1 and 100 years old to the OLF and 10- to 100-year-old C to the HF. The four hurricanes occurred 1, 20, and 29 years before the second data collection point in this study; thus, the two older hurricanes could be the source of a flux of decadal or older C traveling through the OLF and eventually the HF.

4.5 | Synthesis of data on changes to a system under frequent hurricane disturbance

The decrease in mean ages and transit times of soil C over the course of this study could be caused either by dilution, with younger soil C deposited by hurricanes into an inherently older soil C pool, or by increased the loss of older C following hurricanes due to microbial scavenging, or both. We note that loss of older C would likely result from the non-discriminate increase in decomposition from all C pools, but the increased decomposition of very old C would have a disproportionately greater effect on mean bulk soil age and transit time. In surface soils (0-10cm depth) and in the two light fractions, the dilution effect could be explained solely by a recent severe hurricane (e.g., Hurricane Maria in 2017). The dilution hypothesis would be supported by an increase in C stocks, particularly an increase in recently fixed, less-decomposed C. We found an increase in soil C stocks and C:N ratio (see Table S1) of organic matter only in the OLF, not the FLF or HF, suggesting that a dilution effect might occur in the OLF but not in the other two pools. It is possible that our ability to detect small changes in the relatively large FLF and HF pools was limited by the resolution of both soil sampling and analytical procedures (Stanley et al., 2023). Indeed, the depletion of δ^{13} C in all three fractions between 1988 and 2018 indicates either a large influx of less-processed and/or lignin-rich C to the three pools, or that the pools were dominated by rapidly cycling C closely resembling atmospheric levels of δ^{13} C by 2018, supporting dilution with younger C in all three pools. The dilution effect is also supported by stable C and radiocarbon isotopes, as the decrease in the difference of Δ^{14} C from atmospheric concentrations between 1988 and 2018 is consistent with the incorporation of rapidly cycling C.

The microbial scavenging mechanism, whereby microbial decomposition rates do not decrease as quickly as the sudden and prolonged reduction of young inputs, could increase the proportion of old C being decomposed. The slightly higher rate of respiration of very old C would significantly decrease C age and could also explain decreased bulk soil C ages and faster transit times due to hurricanes. The effect of scavenging in soils from 0 to 35 cm depth could be explained by a single recent severe hurricane, while scavenging of mineral-associated C below 35 cm would likely require a regime of repeated severe hurricanes. The FLF and HF C stocks did not increase significantly at any depth between 1988 and 2018, yet their ages and transit times decreased at 35-60 cm. At the 35-60 cm depth, the reduction in 100+ year-old C in OLF and HF pools suggests a loss of older C during the hurricane recovery phase, with century-old C decomposing faster under a regime of severe hurricanes than under constant inputs. The decrease in C concentration of the FLF between 1988 and 2018 (see Supplemental information) could also indicate a higher degree of microbial processing of organic C, consistent with a scavenging effect. Heavy fraction C in this system is associated with redoxactive, iron-rich minerals (Hall et al., 2018; Hall & Silver, 2013). Dramatic soil moisture shifts due to high precipitation influx from hurricanes followed by lower transpiration flux (Miller et al., 2019) may increase iron reduction rates and destabilize mineral-associated C (Barcellos et al., 2018), increasing bioavailability and potentially fueling a large efflux of older C.

5 | CONCLUSIONS

Analysis of soil chemical properties and isotopes before and after four hurricanes in a 30-year period facilitated the examination of the effect of the increasing frequency of hurricanes, including a recent hurricane, on the age and transit time of C through soils.

We found an increase in OLF-C stocks over the study period. Shifts in FLF and mineral-associated HF C stocks were undetectable. The dominance of year- to decades-old C at each depth and fraction, along with a consistently depleted stable C isotope signature, demonstrates the rapid cycling of C through these soils and potentially a significantly increased incorporation of fossil fuel-derived C from the atmosphere into SOC.

Radiocarbon analysis and modeling revealed a mean 20 years decrease in bulk soil age at the 35–60 cm depth. A shift in the age distribution toward younger C under a frequent hurricane scenario, as well as faster transit times in the OLF and HF C pools in surface and 35–60 cm depths, point to the dilution of light fraction C with young C provided by a recent severe hurricane, and a possible loss of older HF C under a regime of multiple hurricanes that could be attributed to increased microbial scavenging of stabilized soil C under post-hurricane microclimates. The increased rate of C cycling, especially of mineral-associated HF C below 35 cm, suggests that increased hurricane frequency has a compounding effect on SOC dynamics, and an increased sensitivity of C previously stabilized in tropical forest soils.

AUTHOR CONTRIBUTIONS

Allegra C. Mayer: Data curation; formal analysis; investigation; project administration; visualization; writing – original draft. Karis J. McFarlane: Conceptualization; funding acquisition; methodology; supervision; writing – review and editing. Whendee L. Silver: Conceptualization; funding acquisition; methodology; supervision; writing – review and editing.

ACKNOWLEDGMENTS

We thank O. Gutierrez del Arroyo, G. Gonzalez, and T. Anthony for generous assistance with sample location and collection; S. Ahmed and Y. Lin for lab assistance and advice; K. Finstad, K. Moreland, and T. Broek for guidance with radiocarbon sample prep; and for running the compact AMS. The manuscript improved thanks to helpful comments from two anonymous reviewers, and from L. Kueppers, M. Torn, and M. Firestone. Research was funded through a Graduate Research Scholarship to A.M. from Lawrence Livermore National Lab and a Department of Energy Office of Science Early Career Award to K.J.M. (SCW1572), as well as NSF Luquillo LTER (DEB-1546686 and DEB-1831952) to the University of Puerto Rico and NSF EAR-2012878 to UC Riverside and EAR-1331841 to the

University of New Hampshire as part of the Critical Zone Program. Additional support was provided by the USDA National Institute of Food and Agriculture, McIntire Stennis project CA-B-ECO-7673-MS, to WLS. A portion of this work was performed under the auspices of the U.S. Department of Energy by Lawrence Livermore National Laboratory under Contract DE-AC52-07NA27344 (LLNL-JRNL-853601). Soil samples were taken from the occupied lands of the Borikén Taíno indigenous people and analyzed on the occupied lands of the Chochenyo-speaking Ohlone people.

CONFLICT OF INTEREST STATEMENT

The authors declare no competing interests.

DATA AVAILABILITY STATEMENT

The data that support the findings of this study are openly available in Dryad at https://doi.org/10.5061/dryad.0k6djhb5k.

ORCID

Allegra C. Mayer https://orcid.org/0000-0003-3408-5906 Karis J. McFarlane https://orcid.org/0000-0001-6390-7863 Whendee L. Silver https://orcid.org/0000-0003-0372-8745

REFERENCES

- Barcellos, D., O'Connell, C. S., Silver, W., Meile, C., & Thompson, A. (2018). Hot spots and hot moments of soil moisture explain fluctuations in iron and carbon cycling in a humid tropical forest soil. *Soil Systems*, 2(4), 59. https://doi.org/10.3390/soilsystems2040059
- Beard, K. H., Vogt, K. A., Vogt, D. J., Scatena, F. N., Covich, A. P., Sigurdardottir, R., Siccama, T. G., & Crowl, T. A. (2005). Structural and functional responses of a subtropical forest to 10 years of hurricanes and droughts. *Ecological Monographs*, 75(3), 345–361. https://doi.org/10.1890/04-1114
- Broek, T. A. B., Ognibene, T. J., McFarlane, K. J., Moreland, K. C., Brown, T. A., & Bench, G. (2021). Conversion of the LLNL/CAMS 1 MV biomedical AMS system to a semi-automated natural abundance ¹⁴C spectrometer: System optimization and performance evaluation. Nuclear Instruments and Methods in Physics Research Section B: Beam Interactions with Materials and Atoms, 499, 124–132. https://doi.org/10.1016/j.nimb.2021.01.022
- Cabugao, K. G., Yaffar, D., Stenson, N., Childs, J., Phillips, J., Mayes, M. A., Yang, X., Weston, D. J., & Norby, R. J. (2021). Bringing function to structure: Root-soil interactions shaping phosphatase activity throughout a soil profile in Puerto Rico. *Ecology and Evolution*, 11(3), 1150–1164. https://doi.org/10.1002/ece3.7036
- Fernandez, I., Mahieu, N., & Cadisch, G. (2003). Carbon isotopic fractionation during decomposition of plant materials of different quality. *Global Biogeochemical Cycles*, 17(3), 1075. https://doi.org/10.1029/2001GB001834
- Finstad, K., van Straaten, O., Veldkamp, E., & McFarlane, K. (2020). Soil carbon dynamics following land use changes and conversion to oil palm plantations in tropical lowlands inferred from radiocarbon. *Global Biogeochemical Cycles*, 34(9), e2019GB006461. https://doi.org/10.1029/2019GB006461
- González, G. (2015). Bisley tower (TOWER I) Meteorological Station ver 63295 [dataset]. Environmental Data Initiative https://doi.org/10.6073/pasta/ac2730ec2c56ffe08302a8c3cc50cd90
- González, G. (2017). Luquillo Mountains meteorological and ceilometer data. Forest Service Research Data Archive. https://doi.org/10.2737/RDS-2017-0023

- Gonzalez, G. (2023). Isley Tower I Meteorological data (Bisley Tower) ver 632957 [dataset]. Environmental Data Initiative. https://doi.org/10.6073/pasta/b082f2cab94810a14456482db686f128
- Guenet, B., Juarez, S., Bardoux, G., Abbadie, L., & Chenu, C. (2012). Evidence that stable C is as vulnerable to priming effect as is more labile C in soil. Soil Biology & Biochemistry, 52, 43–48. https://doi.org/10.1016/j.soilbio.2012.04.001
- Gutiérrez del Arroyo, O., & Silver, W. L. (2018). Disentangling the longterm effects of disturbance on soil biogeochemistry in a wet tropical forest ecosystem. *Global Change Biology*, 24(4), 1673–1684. https://doi.org/10.1111/gcb.14027
- Hall, S. J., Berhe, A. A., & Thompson, A. (2018). Order from disorder: Do soil organic matter composition and turnover co-vary with iron phase crystallinity? *Biogeochemistry*, 140(1), 93–110. https://doi. org/10.1007/s10533-018-0476-4
- Hall, S. J., McNicol, G., Natake, T., & Silver, W. L. (2015). Large fluxes and rapid turnover of mineral-associated carbon across topographic gradients in a humid tropical forest: Insights from paired ¹⁴C analysis. *Biogeosciences*, 12(8), 2471–2487. https://doi.org/10.5194/ bg-12-2471-2015
- Hall, S. J., & Silver, W. L. (2013). Iron oxidation stimulates organic matter decomposition in humid tropical forest soils. Global Change Biology, 19(9), 2804–2813. https://doi.org/10.1111/gcb.12229
- Heartsill-Scalley, T., Scatena, F., Estrada, C., McDowell, W., & Lugo, A. (2007). Disturbance and long-term patterns of rainfall and throughfall nutrient fluxes in a subtropical wet forest in Puerto Rico. *Journal of Hydrology*, 333, 472–485. https://doi.org/10.1016/j.jhydrol.2006. 09.019
- Heartsill Scalley, T., Scatena, F. N., Lugo, A. E., Moya, S., & Estrada Ruiz, C. R. (2010). Changes in structure, composition, and nutrients during 15 Yr of hurricane-induced succession in a subtropical wet forest in puerto rico. *Biotropica*, 42(4), 455–463. Portico. https://doi.org/10.1111/j.1744-7429.2009.00609.x
- Hua, Q., Barbetti, M., & Rakowski, A. (2013). Atmospheric radiocarbon for the period 1950–2010. *Radiocarbon*, 55, 2059–2072. https:// doi.org/10.2458/azu_js_rc.v55i2.16177
- Keeling, C. D. (1979). The Suess effect: ¹³Carbon-¹⁴Carbon interrelations. Environment International, 2(4), 229–300. https://doi.org/10.1016/0160-4120(79)90005-9
- Keeling, R. F., Graven, H. D., Welp, L. R., Resplandy, L., Bi, J., Piper, S. C., Sun, Y., Bollenbacher, A., & Meijer, H. A. J. (2017). Atmospheric evidence for a global secular increase in carbon isotopic discrimination of land photosynthesis. *Proceedings of the National Academy of Sciences of the United States of America*, 114(39), 10361–10366. https://doi.org/10.1073/pnas.1619240114
- Knutson, T., Camargo, S. J., Chan, J. C. L., Emanuel, K., Ho, C.-H., Kossin, J., Mohapatra, M., Satoh, M., Sugi, M., Walsh, K., & Wu, L. (2020). Tropical cyclones and climate change assessment: Part II: Projected response to anthropogenic warming. *Bulletin of the American Meteorological Society*, 101(3), E303–E322. https://doi.org/10.1175/BAMS-D-18-0194.1
- Kossin, J. P., Knapp, K. R., Olander, T. L., & Velden, C. S. (2020). Global increase in major tropical cyclone exceedance probability over the past four decades. *Proceedings of the National Academy of Sciences* of the United States of America, 117(22), 11975–11980. https://doi. org/10.1073/pnas.1920849117
- Kuzyakov, Y., Friedel, J. K., & Stahr, K. (2000). Review of mechanisms and quantification of priming effects. Soil Biology & Biochemistry, 32(11–12), 1485–1498. https://doi.org/10.1016/S0038-0717(00) 00084-5
- Liu, X., Zeng, X., Zou, X., Gonzalez, G., Wang, C., & Yang, S. (2018). Litterfall production prior to and during Hurricanes Irma and Maria in four Puerto Rican forests. *Forests*, 9(6), 367. https://doi.org/10. 3390/f9060367

- Liu, X., Zeng, X., Zou, X., Lodge, D. J., Stankavich, S., González, G., & Cantrell, S. A. (2018). Responses of soil labile organic carbon to a simulated hurricane disturbance in a tropical wet forest. Forests, 9(7), 420. https://doi.org/10.3390/f9070420
- López-Marrero, T., Heartsill-Scalley, T., Rivera-López, C. F., Escalera-García, I. A., & Echevarría-Ramos, M. (2019), Broadening our understanding of hurricanes and forests on the Caribbean Island of Puerto Rico: Where and what should we study now? Forests, 10(9), 710. https://doi.org/10.3390/f10090710
- Manzoni, S., Katul, G. G., & Porporato, A. (2009). Analysis of soil carbon transit times and age distributions using network theories. Journal of Geophysical Research: Biogeosciences, 114(G4). Portico. https:// doi.org/10.1029/2009jg001070
- Marin-Spiotta, E., Silver, W. L., Swanston, C. W., & Ostertag, R. (2009). Soil organic matter dynamics during 80 years of reforestation of tropical pastures. Global Change Biology, 15(6), 1584-1597. https:// doi.org/10.1111/j.1365-2486.2008.01805.x
- McCormack, M. L., Dickie, I. A., Eissenstat, D. M., Fahey, T. J., Fernandez, C. W., Guo, D., Helmisaari, H.-S., Hobbie, E. A., Iversen, C. M., Jackson, R. B., Leppälammi-Kujansuu, J., Norby, R. J., Phillips, R. P., Pregitzer, K. S., Pritchard, S. G., Rewald, B., & Zadworny, M. (2015). Redefining fine roots improves understanding of below-ground contributions to terrestrial biosphere processes. New Phytologist, 207(3), 505-518. https://doi.org/10. 1111/nph.13363
- McDowell, W. H., Scatena, F. N., Waide, R. B., Brokaw, N., Camilo, G. R., Covich, A. P., Crowl, T. A., Gonzalez, G., Greathouse, E. A., Klawinski, P., Lodge, D. J., Lugo, A. E., Pringle, C. M., Richardson, B. A., Richardson, M. J., Schaefer, D. A., Silver, W. L., Thompson, J., Vogt, D. J., ... Zimmerman, J. K. (2012). Geographic and ecological setting of the Luquillo Mountains. In N. Brokaw, T. A. Crowl, A. E. Lugo, W. H. McDowell, F. N. Scatena, R. B. Waide, & M. R. Willig (Eds.), A Caribbean forest tapestry: The multidimensional nature of disturbance and response. Oxford University Press.
- McFarlane, K. J., Torn, M. S., Hanson, P. J., Porras, R. C., Swanston, C. W., Callaham, M. A., & Guilderson, T. P. (2013). Comparison of soil organic matter dynamics at five temperate deciduous forests with physical fractionation and radiocarbon measurements. Biogeochemistry, 112(1), 457-476. https://doi.org/10.1007/s1053 3-012-9740-1
- Miller, P. W., Kumar, A., Mote, T. L., Moraes, F. D. S., & Mishra, D. R. (2019). Persistent hydrological consequences of Hurricane Maria in Puerto Rico. Geophysical Research Letters, 46(3), 1413-1422. https://doi.org/10.1029/2018GL081591
- Murphy, S. F., Stallard, R. F., Scholl, M. A., González, G., & Torres-Sánchez, A. J. (2017). Reassessing rainfall in the Luquillo Mountains, Puerto Rico: Local and global ecohydrological implications. PLoS ONE, 12(7), 1-26. https://doi.org/10.1371/journal. pone.0180987
- Nagy, R. C., Porder, S., Brando, P., Davidson, E. A., Figueira, A. M. E. S., Neill, C., Riskin, S., & Trumbore, S. (2018). Soil carbon dynamics in soybean cropland and forests in Mato Grosso, Brazil. Journal of Geophysical Research: Biogeosciences, 123(1), 18-31. https://doi. org/10.1002/2017JG004269
- Neurath, R. A., Pett-Ridge, J., Chu-Jacoby, I., Herman, D., Whitman, T., Nico, P. S., Lipton, A. S., Kyle, J., Tfaily, M. M., Thompson, A., & Firestone, M. K. (2021). Root carbon interaction with soil minerals is dynamic, leaving a legacy of microbially derived residues. Environmental Science & Technology, 55(19), 13345-13355. https:// doi.org/10.1021/acs.est.1c00300
- Norby, R., Cabugao, K., Yaffar, D., Childs, J., Stenson, N., & Phillips, J. (2019). Root-soil depth profile in Luquillo Experimental Forest, Puerto Rico, February, 2019 [dataset]. Next-Generation Ecosystem Experiments Tropics; Oak Ridge National Laboratory https://doi. org/10.15486/NGT/1574087

- 361-364. R Core Team. (2020). R: A language and environment for statistical computing. R Foundation for Statistical Computing. https://www.R-proje ct.org/
- Rabbi, S. M. F., Minasny, B., McBratney, A. B., & Young, I. M. (2020). Microbial processing of organic matter drives stability and pore geometry of soil aggregates. Geoderma, 360, 114033. https://doi.org/ 10.1016/j.geoderma.2019.114033
- Running, S. W., Nemani, R. R., Heinsch, F. A., Zhao, M., Reeves, M., & Hashimoto, H. (2004). A continuous satellite-derived measure of global terrestrial primary production. Bioscience, 54(6), 547-560. https://doi.org/10.1641/0006-3568(2004)054[0547:ACSMOG] 2.0.CO;2
- Sayer, E. J., Baxendale, C., Birkett, A. J., Bréchet, L. M., Castro, B., Kerdraon-Byrne, D., Lopez-Sangil, L., & Rodtassana, C. (2021). Altered litter inputs modify carbon and nitrogen storage in soil organic matter in a lowland tropical forest. Biogeochemistry, 156(1), 115-130. https://doi.org/10.1007/s10533-020-00747-7
- Sayer, E. J., Powers, J. S., & Tanner, E. V. J. (2007). Increased litterfall in tropical forests boosts the transfer of soil CO₂ to the atmosphere. PLoS ONE, 2(12), e1299. https://doi.org/10.1371/journal.pone. 0001299
- Scatena, F., & Lugo, A. (1995). Geomorphology, disturbance, and the soil and vegetation of two subtropical wet steepland watersheds of Puerto Rico. Geomorphology, 13, 199-213.
- Scatena, F. N. (1989). An introduction to the physiography and history of the Bisley experimental watersheds in the Luquillo Mountains of Puerto Rico.
- Scatena, F. N., & Larsen, M. C. (1991). Physical aspects of hurricane Hugo in Puerto Rico. Biotropica, 23(4), 317-323. https://doi.org/10.2307/
- Scatena, F. N., Moya, S., Estrada, C., & Chinea, J. D. (1996). The first five years in the reorganization of aboveground biomass and nutrient use following hurricane Hugo in the Bisley experimental watersheds, Luquillo experimental Forest, Puerto Rico. Biotropica, 28(4), 424-440. https://doi.org/10.2307/2389086
- Scatena, F. N., Silver, W. L., Siccama, T., Johnson, A., & Sanchez, M. J. (1993). Biomass and nutrient content of the Bisley Experimental Watersheds, Luquillo Experimental Forest, Puerto Rico, before and after hurricane Hugo, 1989. Biotropica, 25(1), 15-27.
- Schrumpf, M., Kaiser, K., Guggenberger, G., Persson, T., Kögel-Knabner, I., & Schulze, E. D. (2013). Storage and stability of organic carbon in soils as related to depth, occlusion within aggregates, and attachment to minerals. Biogeosciences, 10, 1675-1691. https://doi.org/ 10.5194/bg-10-1675-2013
- Sierra, C., Hoyt, A., He, Y., & Trumbore, S. (2018). Soil organic matter persistence as a stochastic process: Age and transit time distributions of carbon in soils. Global Biogeochemical Cycles, 32, 1574-1588. https://doi.org/10.1029/2018GB005950
- Sierra, C. A., Müller, M., & Trumbore, S. E. (2012). Models of soil organic matter decomposition: The SOILR package, version 1.0. Geoscientific Model Development, 5(4), 1045-1060. https://doi.org/ 10.5194/gmd-5-1045-2012
- Sierra, C. A., Müller, M., Metzler, H., Manzoni, S., & Trumbore, S. E. (2017). The muddle of ages, turnover, transit, and residence times in the carbon cycle. Global Change Biology, 23(5), 1763-1773. https:// doi.org/10.1111/gcb.13556

- Sierra, C. A., Müller, M., & Trumbore, S. E. (2014). Modeling radiocarbon dynamics in soils: SoilR version 1.1. *Geoscientific Model Development*, 7(5), 1919–1931. https://doi.org/10.5194/gmd-7-1919-2014
- Silver, W. L., Scatena, F. N., Johnson, A. H., Siccama, T. G., & Sanchez, M. J. (1994). Nutrient availability in a montane wet tropical forest: Spatial patterns and methodological considerations. *Plant and Soil*, 164(1), 129–145. https://doi.org/10.1007/BF00010118
- Silver, W. L., Scatena, F. N., Johnson, A. H., Siccama, T. G., & Watt, F. (1996). At what temporal scales does disturbance affect belowground nutrient pools? *Biotropica*, 28(4), 441–457. https://doi.org/ 10.2307/2389087
- Silver, W. L., & Vogt, K. A. (1993). Fine root dynamics following single and multiple disturbances in a subtropical wet forest ecosystem. *Journal of Ecology*, 81(4), 729–738.
- Soetaert, K., & Petzoldt, T. (2010). Inverse modelling, sensitivity and Monte Carlo analysis in R using package FME. *Journal of Statistical Software*, 33(3), 1–28. https://doi.org/10.18637/jss.v033.i03
- Sollins, P., Kramer, M. G., Swanston, C., Lajtha, K., Filley, T., Aufdenkampe, A. K., Wagai, R., & Bowden, R. D. (2009). Sequential density fractionation across soils of contrasting mineralogy: Evidence for both microbial- and mineral-controlled soil organic matter stabilization. *Biogeochemistry*, 96(1), 209–231. https://doi.org/10.1007/s1053 3-009-9359-z
- Stanley, P., Spertus, J., Chiartas, J., Stark, P. B., & Bowles, T. (2023). Valid inferences about soil carbon in heterogeneous landscapes. *Geoderma*, 430, 116323. https://doi.org/10.1016/j.geoderma. 2022.116323
- Stuiver, M., & Polach, H. A. (1977). Discussion: Reporting of ¹⁴C data. *Radiocarbon*, 19(3), 355–363.
- Swanston, C. W., Torn, M. S., Hanson, P. J., Southon, J. R., Garten, C. T., Hanlon, E. M., & Ganio, L. (2005). Initial characterization of processes of soil carbon stabilization using forest stand-level radiocarbon enrichment. *Geoderma*, 128(1–2), 52–62. https://doi.org/10. 1016/j.geoderma.2004.12.015
- Thomas, G. W. (1996). Soil pH and soil acidity. In D. L. Sparks, A. L. Page,
 P. A. Helmke, R. H. Loeppert, P. N. Soltanpour, M. A. Tabatabai, C.
 T. Johnston, & M. E. Sumner (Eds.), SSSA Book Series (pp. 475-490).
 Soil Science Society of America, American Society of Agronomy.
 https://doi.org/10.2136/sssabookser5.3.c16
- Throop, H. L., Archer, S., Monger, H. C., & Waltman, S. (2012). When bulk density methods matter: Implications for estimating soil organic carbon pools in rocky soils. *Journal of Arid Environments*, 77, 66–71. https://doi.org/10.1016/j.jaridenv.2011.08.020
- Trumbore, S. (2000). Age of soil organic matter and soil respiration: Radiocarbon constraints on belowground C dynamics. *Ecological Applications*, 10(2), 399–411. https://doi.org/10.1890/1051-0761(2 000)010[0399:AOSOMA]2.0.CO;2
- Trumbore, S. E. (1993). Comparison of carbon dynamics in tropical and temperate soils using radiocarbon measurements. *Global Biogeochemical Cycles*, 7(2), 275–290. https://doi.org/10.1029/93GB00468
- Trumbore, S. E., Davidson, E. A., de Camargo, P., Nepstad, D. C., & Martinelli, L. A. (1995). Belowground cycling of carbon in forests

- and pastures of eastern Amazonia. Global Biogeochemical Cycles, 9(4), 515-528. https://doi.org/10.1029/95GB02148
- Vogel, J. S., Southon, J. R., Nelson, D. E., & Brown, T. A. (1984). Performance of catalytically condensed carbon for use in accelerator mass spectrometry. *Nuclear Instruments and Methods in Physics Research B*, 5(2), 289–293. https://doi.org/10.1016/0168-583X(84) 90529-9
- Vogt, K. A., Vogt, D. J., Boon, P., Covich, A., Scatena, F. N., Asbjornsen, H., O'Harra, J. L., Perez, J., Siccama, T. G., Bloomfield, J., & Ranciato, J. F. (1996). Litter dynamics along stream, riparian and upslope areas following Hurricane Hugo, Luquillo Experimental Forest, Puerto Rico. *Biotropica*, 28(4), 458–470. https://doi.org/10.2307/2389088
- Weaver, P. L., & Murphy, P. G. (1990). Forest structure and productivity in Puerto Rico's Luquillo Mountains. *Biotropica*, 22(1), 69–82. https://doi.org/10.2307/2388721
- Wu, Z., Dijkstra, P., Koch, G. W., Penuelas, J., & Hungate, B. A. (2011). Responses of terrestrial ecosystems to temperature and precipitation change: A meta-analysis of experimental manipulation. Global Change Biology, 17(2), 927-942. https://doi.org/10.1111/j.1365-2486.2010.02302.x
- Yaffar, D., & Norby, R. J. (2020). A historical and comparative review of 50 years of root data collection in Puerto Rico. *Biotropica*, *52*(3), 563–576. https://doi.org/10.1111/btp.12771
- Yaffar, D., Wood, T. E., Reed, S. C., Branoff, B. L., Cavaleri, M. A., & Norby, R. J. (2021). Experimental warming and its legacy effects on root dynamics following two hurricane disturbances in a wet tropical forest. Global Change Biology, 27(24), 6423–6435. https://doi.org/ 10.1111/gcb.15870
- Zeikus, J. G. (1981). Lignin metabolism and the carbon cycle. In M. Alexander (Ed.), *Advances in microbial ecology* (pp. 211–243). Springer US. https://doi.org/10.1007/978-1-4615-8306-6_5
- Zuur, A. F., Ieno, E. N., Walker, N. J., Saveliev, A. A., & Smith, G. M. (2009). Mixed effects modelling for nested data. *Mixed effects models and extensions in ecology with R* (pp. 101–142). Springer. https://doi.org/10.1007/978-0-387-87458-6_5

SUPPORTING INFORMATION

Additional supporting information can be found online in the Supporting Information section at the end of this article.

How to cite this article: Mayer, A. C., McFarlane, K. J., & Silver, W. L. (2024). The effect of repeated hurricanes on the age of organic carbon in humid tropical forest soil. *Global Change Biology*, 30, e17265. https://doi.org/10.1111/gcb.17265